

AD-A164 492

AN ANALYSIS OF THE PERFORMANCE OF THE FANS OF A WIND
TUNNEL AT THE NAVAL POSTGRADUATE SCHOOL(U) NAVAL
POSTGRADUATE SCHOOL MONTEREY CA M L PEREIRA DEC 85

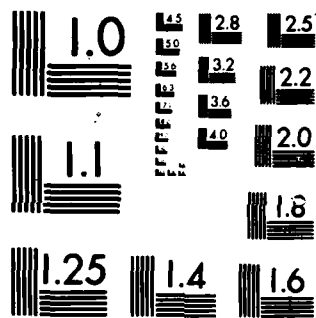
1/1

UNCLASSIFIED

F/G 20/4

NL

END



MICROCOPY RESOLUTION TEST CHART
NATIONAL BUREAU OF STANDARDS-1963-A

2

NAVAL POSTGRADUATE SCHOOL

Monterey, California

AD-A164 492



DTIC
ELECTE
FEB 26 1986
S D
D
D

THESIS

AN ANALYSIS OF THE PERFORMANCE OF
THE FANS OF A WIND TUNNEL AT THE
NAVAL POSTGRADUATE SCHOOL

Pereira, Marcos Luis

December 1985

Thesis Advisor:

J. V. Healey

Approved for public release; distribution is unlimited.

DTIC FILE COPY

36 2 25 029

AD-A164492

SECURITY CLASSIFICATION OF THIS PAGE

REPORT DOCUMENTATION PAGE

1a. REPORT SECURITY CLASSIFICATION		1b. RESTRICTIVE MARKINGS	
2a. SECURITY CLASSIFICATION AUTHORITY		3. DISTRIBUTION / AVAILABILITY OF REPORT Approved for public release; distribution is unlimited.	
2b. DECLASSIFICATION / DOWNGRADING SCHEDULE			
4. PERFORMING ORGANIZATION REPORT NUMBER(S)		5. MONITORING ORGANIZATION REPORT NUMBER(S)	
6a. NAME OF PERFORMING ORGANIZATION Naval Postgraduate School	6b. OFFICE SYMBOL (If applicable) Code 67	7a. NAME OF MONITORING ORGANIZATION Naval Postgraduate School	
6c. ADDRESS (City, State, and ZIP Code) Monterey, California 93943		7b. ADDRESS (City, State, and ZIP Code) Monterey, California 93943	
8a. NAME OF FUNDING / SPONSORING ORGANIZATION	8b. OFFICE SYMBOL (If applicable)	9. PROCUREMENT INSTRUMENT IDENTIFICATION NUMBER	
8c. ADDRESS (City, State, and ZIP Code)		10. SOURCE OF FUNDING NUMBERS	
		PROGRAM ELEMENT NO.	PROJECT NO.
		TASK NO.	WORK UNIT ACCESSION NO.

11 TITLE (Include Security Classification) AN ANALYSIS OF THE PERFORMANCE OF THE FANS OF A WIND TUNNEL AT THE NAVAL POSTGRADUATE SCHOOL

12 PERSONAL AUTHOR(S) Pereira, Marcos Luis

13a TYPE OF REPORT Master's Thesis	13b TIME COVERED FROM _____ TO _____	14 DATE OF REPORT (Year, Month, Day) 1985 December	15 PAGE COUNT 94
---------------------------------------	---	---	---------------------

16 SUPPLEMENTARY NOTATION

17 COSATI CODES			18 SUBJECT TERMS (Continue on reverse if necessary and identify by block number) Wind tunnel blades
FIELD	GROUP	SUB-GROUP	

19 ABSTRACT (Continue on reverse if necessary and identify by block number)

The large subsonic "academic" wind tunnel at NPS, powered by two counter-rotating fans, never achieved the design specifications. The reason for the poor performance of the tunnel was unknown but believed to be due to either poorly designed fan blades or to separation in the diffuser. Being easier to analyze, the fan blades were chosen for initial study.

The approach used is a new blade element method for calculating the performance of high and intermediate solidity fans. Although this new method predicts some deviations from the original isolated blade analysis, it was

20 DISTRIBUTION / AVAILABILITY OF ABSTRACT <input checked="" type="checkbox"/> UNCLASSIFIED/UNLIMITED <input type="checkbox"/> SAME AS RPT <input type="checkbox"/> DTIC USERS	21 ABSTRACT SECURITY CLASSIFICATION Unclassified
---	---

22a NAME OF RESPONSIBLE INDIVIDUAL J. V. Healey	22b TELEPHONE (Include Area Code) (408 646-2804	22c OFFICE SYMBOL Code 67X1
--	--	--------------------------------

Block 3. (continued)

found that the design was adequate and, therefore, the tunnel problem is most probably due to separation in the diffuser.



Approved for public release; distribution is unlimited.

An Analysis of the Performance of
the Fans of a Wind Tunnel at the
Naval Postgraduate School

by

Pereira, Marcos Luis
Lt. Col. Brazilian Air Force
B.S., Mechanical Engineering, Instituto Tecnológico da
Aeronautica, Sao Paulo, Brasil

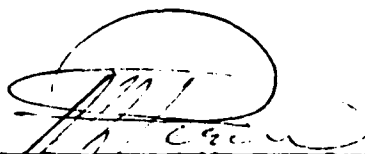
Submitted in partial fulfillment of the
requirements for the degree of

MASTER OF SCIENCE IN AERONAUTICAL ENGINEERING

from the

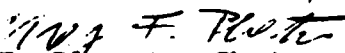
NAVAL POSTGRADUATE SCHOOL
December 1985

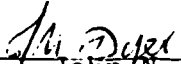
Author:


Pereira, Marcos Luis

Approved by:


J. V. Healey, Thesis Advisor


Max F. Platzer, Chairman,
Department of Aeronautics


John N. Dyer,
Dean of Science and Engineering

ABSTRACT

The large subsonic "academic" wind tunnel at NPS, powered by two counter-rotating fans, never achieved the design specifications. The reason for the poor performance of the tunnel was unknown but believed to be due to either poorly designed fan blades or to separation in the diffuser. Being easier to analyse, the fan blades were chosen for initial study.

The approach used is a new blade element method for calculating the performance of high and intermediate solidity fans. Although this new method predicts some deviations from the original isolated blade analysis, it was found that the design was adequate and, therefore, the tunnel problem is most probably due to separation in the diffuser.

TABLE OF CONTENTS

I. INTRODUCTION 11

II. EVALUATION OF LOSSES 13

 A. INTRODUCTION 13

 B. CYLINDRICAL SECTIONS 16

 1. Test Section 16

 2. Fan Duct Losses 17

 3. Constant Area Ducts 17

 C. DIFFUSERS 17

 1. First Diffuser 18

 2. Second Diffuser 20

 D. CONTRACTION CONE 21

 E. SPINNER 21

 F. CORNERS 22

 G. SUMMARY OF LOSSES 24

III. BLADE PERFORMANCE 28

 A. INTRODUCTION 28

 B. THE LARSON REPORT 28

 C. THE BORST METHOD 30

 D. TORQUE AND POWER EVALUATION 31

 E. INTERACTION BETWEEN STAGES 35

 F. CONCLUSION 38

IV. TUNNEL PERFORMANCE 56

 A. INTRODUCTION 56

 B. TUNNEL LOSSES 56

 C. OPERATIONAL ENVELOPE 56

 D. FINAL CONCLUSION 59

M
□
□

Availability Codes	
Dist	Avail and/or Special
A-1	



APPENDIX A: SPECIFIED FUNCTIONAL FORMS	64
APPENDIX B: SAMPLE CALCULATIONS	66
APPENDIX C: DESCRIPTION OF COMPUTER PROGRAMS	69
APPENDIX D: COMPUTER PROGRAM 'LOSS'	71
APPENDIX E: COMPUTER PROGRAM 'BORST'	75
LIST OF REFERENCES	87
INITIAL DISTRIBUTION LIST	88

LIST OF TABLES

I	PARAMETERS FOR DIFFUSER 1	19
II	PARAMETERS FOR EACH PART OF DIFFUSER 1	20
III	PARAMETERS FOR EACH PART OF DIFFUSER 2	20
IV	PARAMETERS OF CORNERS	23
V	CORNER LOSSES BY PANKHURST AND HOLDER	25
VI	LOSS FOR EACH SECTION OF TUNNEL AT VO=200 KNOTS	26
VII	TUNNEL LOSS BY THREE METHODS	27
VIII	VELOCITIES AT EACH STATION, FIRST STAGE, VO=200 KNOTS	43
IX	REYNOLDS AND MACH NUMBERS AT EACH BLADE STATION, FIRST STAGE, VO=200 KNOTS	44
X	ANGLES AT EACH STATION, FIRST STAGE, VO=200 KNOTS	45
XI	CORRECTED LIFT AND DRAG COEFFICIENT, LIFT AND TORQUE, FIRST STAGE, VO= 200 KNOTS	46
XII	VELOCITIES AT EACH STATION, SECOND STAGE, VO=200 KNOTS	47
XIII	REYNOLDS AND MACH NUMBER AT EACH STATION, SECOND STAGE, VO= 200 KNOTS	48
XIV	ANGLES AT EACH STATION, SECOND FAN STAGE, VO=200 KNOTS	49
XV	CORRECTED LIFT AND DRAG COEFFICIENT, BETA1-BETA4, AT EACH STATION, SECOND STAGE, VO=200 KNOTS	50
XVI	ANGLES, LIFT AND DRAG COEF. AT EACH STATION WITHOUT CORRECTION OF ANGLE OF ATTACK, FIRST STAGE, VO=200 KNOTS	51
XVII	LIFT, RESULTANT FORCE AND TORQUE WITHOUT CORRECTION OF ANGLE OF ATTACK, FIRST STAGE, VO= 200 KNOTS	52
XVIII	VELOCITIES AT EACH STATION WITHOUT CORRECTION OF ANGLE OF ATTACK, SECOND STAGE, VO=200 KNOTS	53
XIX	ANGLES, LIFT AND DRAG COEF. AT EACH STATION WITHOUT CORRECTION OF ANGLE OF ATTACK, SECOND STAGE, VO=200 KNOTS	54
XX	LIFT, RESULTANT FORCE AND TORQUE, SECOND STAGE WITHOUT CORRECTION OF ANGLE OF ATTACK, VO=200 KNOTS	55

XXI	OPERATIONAL ENVELOPE FOR EQUATION 4.1	60
XXII	OPERATIONAL ENVELOPE FOR EQUATION 4.2	62

LIST OF FIGURES

2.1	Partition of Tunnel Circuit for Evaluation of Losses	14
2.2	Spinner Dimensions	22
3.1	Angle of Attack Relations	32
3.2	Lift Developed at Each Blade Station	34
3.3	Sketch for Torque Evaluation at Each Station	36
3.4	Axial Flow Velocity Triangles	37
3.5	Tangential Force on the Blade at Each Station Vo=200 Knots, Pitch Angle= 2.4 degrees	41
3.6	Corrected and Uncorrected Angle of Attack Vo=200 Knots, Pitch Angle= 2.4 degrees	42
4.1	Energy Required to Overcome Tunnel Losses	57
4.2	Operational Envelope for Equation 4.1	61
4.3	Operational Envelope for Equation 4.2	63

ACKNOWLEDGEMENT

To my wife, Graciete, and my children, Tereza, Tais, Carlsbad and Tulio for their love and support through out this work.

I. INTRODUCTION

The "academic" wind tunnel at NPS is inadequate for most tasks, due to the excessive level of turbulence at high speed. This tunnel was designed for a potential speed of 200 Knots in the test section, but this value has not been reached yet. This project was undertaken with the purpose of evaluating, by a different method from that used for designing, the performance of the tunnel in order to establish possible causes of the problem.

The two counter - rotating fans could be the cause of the trouble since they were designed using a blade element theory, that does not take account of the three dimensional effects that are present at medium and high solidities. These effects cause changes in the apparent velocity vector, therefore the blades were analysed by a " New Blade Element Method for Calculating the Performance of High and Intermediate Solidity Axial Flow Fans " due to Borst [Ref. 1: p.1]. This method determines an induced angle of attack which changes the apparent velocity past the airfoil and it has been found to be a reliable measure of the three dimensional effects. The data required for this method comes from the two dimensional airfoil data, that is available in the current literature. This method was used in reference 1 (p.10) assuming zero drag, and the predictions showed excellent agreement with measurements. The small difference between the results can be attributed to the assumption of zero drag. The performance of the first and second stage blades of the academic wind tunnel is evaluated assuming non zero drag, so it is expected that the results will be realistic.

A possible cause of the inability to reach the specified speed could be excessive losses around the tunnel circuit, principally at the first diffuser and the corners. The first

diffuser has a high angle of divergence which can provide a flow separation, further losses and turbulence. The evaluation of losses around the tunnel is made by means of the method given by RAE & POPE [Ref. 2: p.87], which breaks the tunnel down into sections and calculates the losses for each one. The four corner losses are evaluated by three methods:

- 1 considering one third of the losses due to skin friction and two third losses due to rotation; an empirical relation given by RAE & POPE [Ref. 2: p.90], was used to account for the different types of corner vane,
- 2 considering empirical values found by testing and
- 3 considering variation of resistance coefficient with gap/chord ratio of thin corner vanes given by PANKHURST & HOLDER [Ref. 3: p.93].

The first diffuser, since it has variable divergence, was broken into four parts and the losses evaluated part by part through the method given by RAE & POPE [Ref. 2: p.89], this shows that the losses are strongly dependent on the diffuser angle.

After all losses were evaluated , a relation between the air inflow velocity to the blades and the power output from the blades is found and the non-stall operation envelope is determined. The temperature and pressure assumed by LARSON in the original blade design [Ref. 4: p.5], are $T = 100^{\circ} \text{ F}$ $p = 2,246 \text{ (lb/ft}^2 \text{)}$ and, therefore the values of kinematic viscosity (ν) of $0.000166 \text{ (ft}^2 \text{ / sec)}$ and sound velocity of 1160 ft /sec , as presented in Appendix C, will be used for evaluation of the Reynolds and Mach numbers.

II. EVALUATION OF LOSSES

A. INTRODUCTION

As mentioned in chapter one, we will use the procedure outlined by RAE & POPE [Ref. 2: p.87], that consists of breaking the tunnel down into cylindrical sections, expanding sections, contracting sections and corners, in order to evaluate the tunnel losses.

The sections are numbered in such way that those sections with the same characteristics, that is, those that use the same loss equation, are kept together. This facilitates the evaluation by computer. Then, the cylindrical sections are numbered from 1 to 4, the expanding sections from 5 to 11, the contracting section and spinner take the number 12 and 13 respectively, and finally the corners from 14 to 17.

The Figure 2.1 shows the sections and their designated numbers, as they are discriminated below:

SECTION	DISCRIMINATION
1	test section
2	fan duct
3	constant area duct
4	constant area duct
5	first diffuser (sec 1)
6	" diffuser (sec 2)
7	" diffuser (sec 3)
8	" diffuser (sec 4)
9	second diffuser (sec 1)
10	" diffuser (sec 2)
11	" diffuser (sec 3)
12	contraction cone
13	spinner
14	first corner with full size vanes

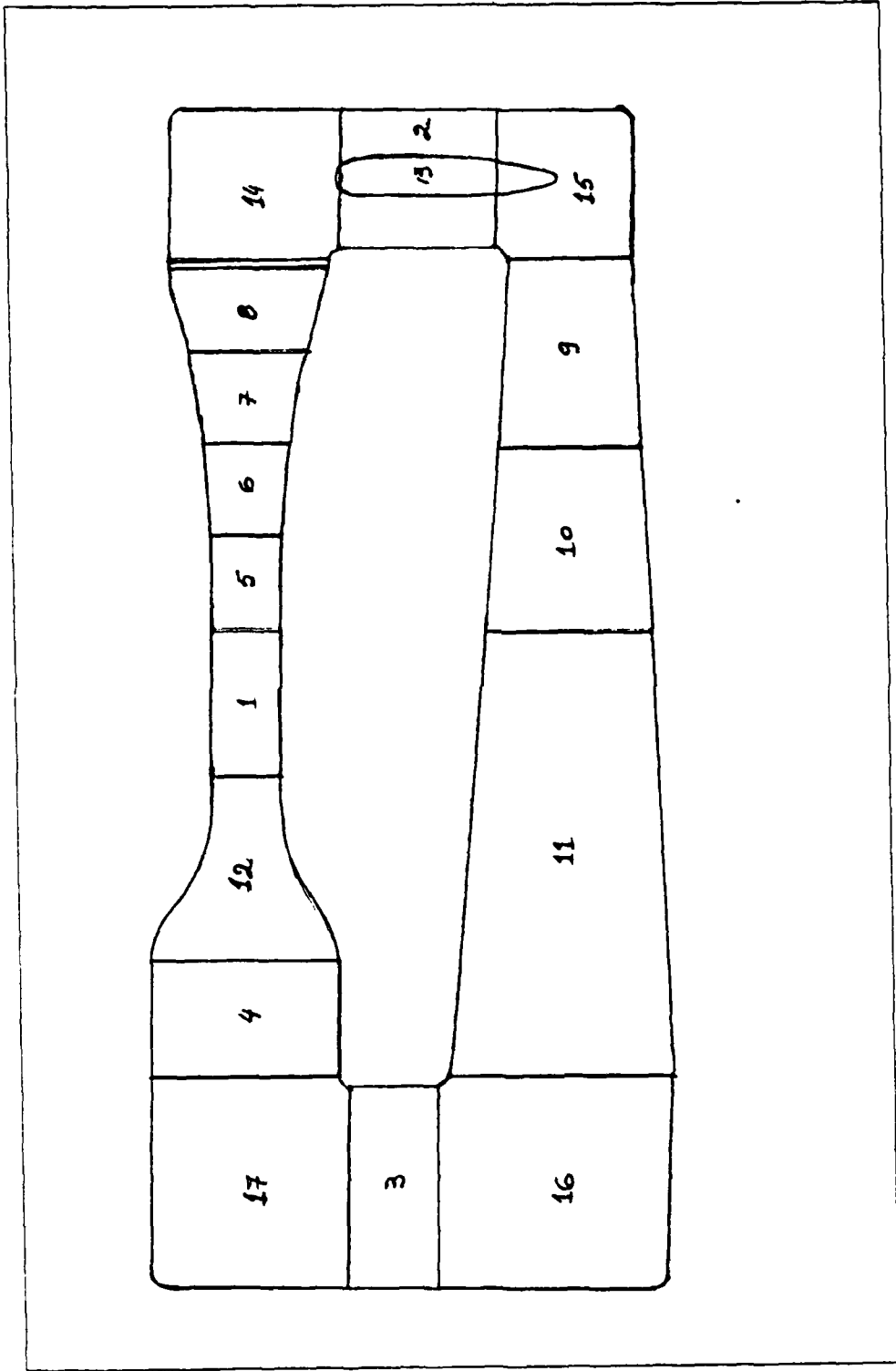


Figure 2.1 Partition of Tunnel Circuit for Evaluation of Losses.

- 15 second corner with full size vanes
- 16 third corner with full size vanes
- 17 fourth corner with half size vanes

The dimensions of the sections, which are used for evaluating the losses, are taken from a WEST COAST RESEARCH CO. drawing [Refs. 7,8].

In each section the loss K will be a drop in static pressure divided by the dynamic pressure at that section, as given by RAE & POPE [Ref. 2: p.87] and rewritten below

$$K_o = K(q/q_o),$$

$$K = (p_i - p_f) / q \text{ loss at each section,}$$

$$K_o = \text{coefficient of loss related to test section,}$$

$$p_i = \text{inlet section pressure,}$$

$$p_f = \text{outlet section pressure,}$$

$$q = \text{dynamic pressure at section,}$$

$$q_o = \text{dynamic pressure at test section.}$$

In terms of diameter we get

$$K_o = K(D_o/D), \text{ where}$$

$$D_o = \text{test section diameter,}$$

$$D = \text{local tunnel diameter,}$$

and finally, for energy ratio of the tunnel,

$$E_{RT} = \text{jet energy/summation of circuit losses.}$$

The losses are evaluated by means of a computer program written in FORTRAN IV language, which is presented in Appendix A, and named LOSS.

When the evaluation of skin friction is needed, it is made by subroutine FRIC in the LOSS program, using the equation from RAE & POPE [Ref. 2: p.88], shown immediately below,

$$1/\lambda = 2 \log_{10} \text{Re} \lambda - 0.8, \quad (\text{eqn 2.1})$$

where λ = skin friction coefficient and Rey = Reynolds number.

The Reynolds number at each section is related to Reynolds number at the test section, as follows:

$$Rey = VD/\nu .$$

From the continuity equation $AV = A_o V_o$, and hence

$Rey = (D_o/\nu)V_o(D_o/D)$, from which is found

$$Rey = 2.63E 04 V_o(D_o/D) . \quad (\text{eqn 2.2})$$

B. CYLINDRICAL SECTIONS

1. Test Section

The losses for this octagonal section are evaluated through the eqn 2.3, (eqn 2.44, Ref. 2, p.88) for the equivalent cylindrical section,

$$K_o = \lambda(L /D_e)(D_o/D_e)^4, \quad (\text{eqn 2.3})$$

where D_e is the diameter of the circle whose circumference equals the perimeter of the octagon.

Then, the dimensions for the test section are:

$$\begin{aligned} \text{Length} &= 8.00 \text{ feet,} \\ \text{Diameter} &= 4.36 \text{ feet.} \end{aligned}$$

This diameter is the test section diameter (D_o) used in all the equations related to the test section.

The losses for the test section at each velocity are calculated by the computer program LOSS using the equations below, which were obtained from eqn 2.3, from the equation of the Reynolds number, and from the dimensions above.

$$\text{section 1: } K_o = 1.834\lambda , \text{ } Rey = 2.63E 04 V_o .$$

2. Fan Duct Losses

This section begins after the first corner with a octagonal cross section, changes to a cylindrical section where the two stages operate and ends in another octagonal section. From an original wind tunnel drawing (Ref. 8) we have the dimensions for this section and, using the same procedure as above (test section), we get the following dimensions:

$$De = 7.50 \text{ ft} \quad L = 9.50 \text{ ft} .$$

The same equations used for test section are used here and the equations for the computer program are:

$$\text{section 2: } Ko = .1448\lambda , \text{ Rey} = 1.54E 04 \text{ Vo} .$$

3. Constant Area Ducts

The losses are evaluated in the same manner as for the test section . The dimensions for these two ducts are:

$$\text{section 3: } De = 13.37 \text{ ft}, \quad L = 6.00 \text{ ft} .$$

$$\text{section 4: } De = 12.73 \text{ ft}, \quad L = 6.34 \text{ ft} .$$

The equations for the computer program are:

$$\text{section 3: } Ko = .0051\lambda , \quad \text{Rey} = .86E 04 \text{ Vo} .$$

$$\text{section 4: } Ko = .0067\lambda , \quad \text{Rey} = .90E 04 \text{ Vo} .$$

C. DIFFUSERS

The diffusers are broken down into parts, the first (between test section and first corner) into four, and the second (between the second and third corners) into three, the purpose of which is to make the evaluation of losses more accurately. The diffuser divergence angle, which strongly affects the evaluation, is taken for each part as the difference between the equivalent small and large diameters, divided by the length.

The equation used comes from RAE & POPE [Ref. 2: p.89], and it is

$$K_o = A (\lambda/8 \tan(\alpha/2) + .6 \tan(\alpha/2)), \quad (\text{eqn 2.4})$$

where $A = (1 - (D1/D2)^4)(D_o/D1)^4$, and

λ = skin friction coefficient for Reynolds number given by eqn 2.2, and based on the mean diameter,

α = divergence angle between walls,

D_o = test section diameter,

$D1$ = smaller diameter of diffuser,

$D2$ = larger diameter of diffuser.

1. First Diffuser

The diffuser cross section from the test section to the first corner varies along its 20 feet of length, and its height H and width W are given as a function of the distance X (ft), along the flow axis, by the equations:

$$H = 3.52 + .00440 X^{2.4} \text{ (ft)}, \quad (\text{eqn 2.5})$$

$$W = 5.02 + .00036 X^3 \text{ (ft)}. \quad (\text{eqn 2.6})$$

Furthermore, its cross-sectional area is:

$$\text{Area} = .828 W H \text{ (ft}^2 \text{)}.$$

The following table gives the local values of H, W, Area and D_e as function of X for this diffuser, where

D_e = equivalent local section diameter (ft).

The evaluation of the diffuser angle is made by the following equations:

-For the divergence angle of the equivalent conical diffuser

-For the divergence angle between the walls in the

TABLE I
PARAMETERS FOR DIFFUSER 1

X	H	W	Area	De
0	3.52	5.02	14.63	4.32
5.0	3.73	5.06	15.64	4.46
10.0	4.62	5.38	20.60	5.12
15.0	6.44	6.28	33.27	6.51
18.7	8.50	7.38	51.94	8.13

$$\alpha = 2 \arctan((D_2 - D_1)/2L) \quad . \quad (\text{eqn 2.7})$$

vertical and horizontal planes respectively:

$$\alpha_h = \arctan((h_2 - h_1)/2L), \quad (\text{eqn 2.8})$$

$$\alpha_w = 2 \arctan((w_2 - w_1)/2L), \quad (\text{eqn 2.9})$$

where indexes 1 and 2 refer to small and large local sections and L is the length between them.

For the first diffuser, the equations 2.8 and 2.9 are used because the angles between the walls are different, as shown in Table II .

For a conservative analysis, the larger values are chosen in computing the loss coefficient K_o .

With the dimensions from this table and the equations 2.4 and 2.2 we got the following equations to use with the computer program LOSS :

TABLE II
PARAMETERS FOR EACH PART OF DIFFUSER 1

Part	L(ft)	D1(ft)	D2(ft)	α_w (deg.)	α_h (deg.)
1	5.0	4.36	4.46	0.52	2.29
2	5.0	4.46	5.12	3.60	10.23
3	5.0	5.12	6.51	9.77	20.63
4	3.7	6.51	8.13	17.50	30.85

section 5: $Ko = .5367\lambda + .00103$, $Re_y = 2.60E 04 Vo.$

section 6: $Ko = .5416\lambda + .0208$, $Re_y = 2.40E 04 Vo.$

section 7: $Ko = .2232\lambda + .0355$, $Re_y = 1.97E 04 Vo.$

section 8: $Ko = .0540\lambda + .0196$, $Re_y = 1.57E 04 Vo.$

2. Second Diffuser

For the second diffuser, the values of D1 and D2 are substituted into equation 2.7 for evaluation of the divergence angle, because the angles between the walls in the vertical and horizontal planes have no large difference.

TABLE III
PARAMETERS FOR EACH PART OF DIFFUSER 2

Part	L	D1	D2	α
1	9.97	7.40	7.88	2.76
2	9.97	7.88	8.89	5.79
3	24.10	8.89	14.01	12.10

With the dimensions on Table III and equations 2.4 and 2.2, we got the following equations to use with the computer program LOSS.

section 9 : $Ko = .14\lambda + .0004$, $Rey = 1.50E\ 04\ Vo.$
 section 10: $Ko = .09\lambda + .0011$, $Rey = 1.37E\ 04\ Vo.$
 section 11: $Ko = .05\lambda + .0030$, $Rey = 1.00E\ 04\ Vo.$

D. CONTRACTION CONE

This section takes the number 12; it is located between corner four and the test section. The equation used is from RAE & POPE [Ref. 2: p.91], and is

$$Ko = .32\lambda Lc/Do, \quad (\text{eqn 2.10})$$

where λ = skin friction coefficient for the Reynolds number given by eqn 2.2 with $D = (D1 + D2)/2$; Lc = length of contraction cone.

The equations for the computer program are:

section 12: $Ko = .7338\lambda$, $Rey = 1.34E\ 04\ Vo.$

E. SPINNER

This section takes the number 13, and it is located in the fan duct. The dimensions are shown in fig 2.2 and the loss is evaluated using a method given by Nicolai [Ref. 10: p.11-21]. The following equations are for use with the computer program:

$$\begin{aligned}
 Rel &= 2.45E-04\ Vo, \\
 Cdf &= .455 / (\log_{10} Rel), \\
 Cdo &= Cdf + .000616 / Cdf, \\
 Ko &= .00837\ Cdo, \\
 Cdo &= \text{drag coefficient}, \\
 Cdf &= \text{friction drag coefficient},
 \end{aligned}$$

where Rel = Reynolds Number related to body diameter.

The dimensions are :

$$\begin{aligned}
 L &= \text{Length} = 12.0\ \text{ft}, \\
 D &= \text{Body diameter} = 2.0\ \text{ft}, \\
 Db &= \text{Base body diameter} = 0.554\ \text{ft}.
 \end{aligned}$$

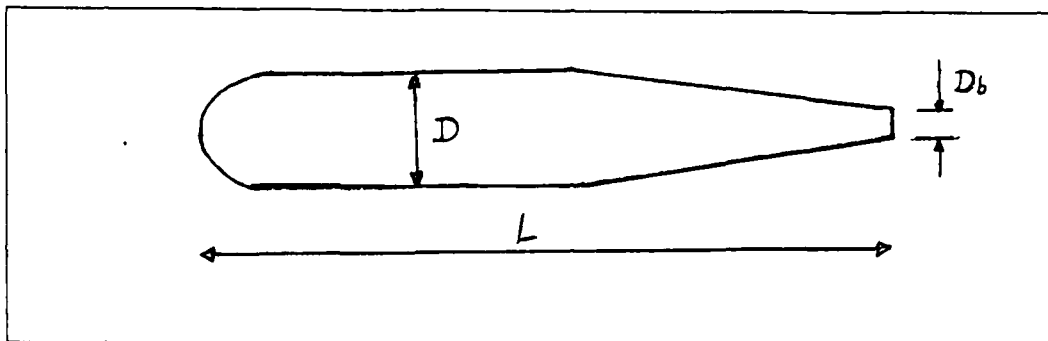


Figure 2.2 Spinner Dimensions.

F. CORNERS

The corners are evaluated in three different ways:

- (i) RAE & POPE [Ref. 2: pp.89,90].
- (ii) Bradshaw and Pankhurst [Ref. 5: p.29].
- (iii) Pankhurst and Holder [Ref. 3: p.90].

By RAE & POPE the loss equation is

$$K_o = (0.1 + (4.55 / (\log_{10} R_n)^{2.58})) (D_o / D)^4, \quad (\text{eqn 2.11})$$

where R_n = Reynolds number based on chord vane,

D = equivalent diameter of inlet cross section.

The dimensions are in Table IV.

With the dimensions from Table IV and the eqn 2.11, the equations to be used in the computer program are found and are as follow:

section 14: $K_o = .00690 + .3122 / (\log_{10} R_n)^{2.58},$
 $Re_y = 1.646E 03 V_o .$

section 15: $K_o = .00905 + .4118 / (\log_{10} R_n)^{2.58},$
 $Re_y = 1.890E 03 V_o .$

section 16: $K_o = .00094 + .0428 / (\log_{10} R_n)^{2.58},$
 $Re_y = .609E 03 V_o .$

section 17: $K_o = .00113 + .0515 / (\log_{10} R_n)^{2.58},$
 $Re_y = .334E 03 V_o .$

TABLE IV
PARAMETERS OF CORNERS

Section	Chord(ft)	D(ft)
14	1.042	8.52
15	1.042	7.95
16	1.042	14.00
17	0.521	13.37

From Bradshaw and Pankhurst, an empirical equation based on tests at Reynolds number $2.0E+05$ and $1.9E+06$, gives the loss coefficient as

$$C_p = 1.2 (Uc/\nu)^{-.25} , \quad (\text{eqn 2.12})$$

where U = local flow velocity,
 c = vane chord,
 ν = kinematic viscosity.

This equation, when related to the test section velocity by means of equation $K_o = C_p (D_o/D)^4$ yields the following equations for use with the computer program.

section 14: $K_o = .0130 V_o^{-.25} ,$
 section 15: $K_o = .0160 V_o^{-.25} ,$
 section 16: $K_o = .0023 V_o^{-.25} ,$
 section 17: $K_o = .0032 V_o^{-.25} .$

Pankhurst and Holder's method is a graphic one, which gives the variation of loss coefficient with the gap/chord ratio of the vanes. The tunnel we are dealing with has corner - vane sections similar to type b of figure 40 of reference 3. Taking the dimensions of the corners and vanes from the drawing, evaluating the gap/chord ratio for each corner and entering the graph on page 93 of reference 3 , the value of K (C is used in Pankhurst & Holder) is found,

and used with the equations below:

$$K = 2 \nabla H / \rho U^2 , \quad (\text{eqn 2.13})$$

$$K_o = K (D_o/D)^4 , \quad (\text{eqn 2.14})$$

where U = local velocity at entry of corner,

∇H = drop of pressure across the corner,

D = equivalent corner diameter at entry,

K = loss coefficient from the graph.

Sample calculations

For corner # 1 we have

$$\text{gap / chord} = (8.36 - 2.48) / 12.5 = 0.4704,$$

$$(D_o/D)^4 = 0.0967,$$

$$K = 0.235,$$

$$K_o = 0.0227.$$

The losses in all four corners, as given by Pankhurst and Holder's method are shown in Table V .

G. SUMMARY OF LOSSES

The losses evaluated by the computer program for sections 1 through 17 for a test section velocity of 200 Knots, are shown in Table VI ; values for velocities from 100 to 200 Knots are shown in Table VII .

The energy ratio given by Ert is multiplied by .9 in order to take into account the losses due to leaks and joints.

The results presented in Table VII include, for purposes of comparison, the losses evaluated by the other two methods. At the design airspeed of 200 Knots, Pankhurst &

TABLE V
CORNER LOSSES BY PANKHURST AND HOLDER

corner	gap/chord	$(D_o/D)^4$	K	Ko
1	0.4704	0.0967	0.23	0.023
2	0.4256	0.1334	0.27	0.036
3	0.4752	0.0094	0.23	0.002
4	0.4656	0.0113	0.24	0.003

Holder's method predicts that 245 HP will be required, while Bradshaw & Pankhurst (a later work) indicates a need for 170 HP. Rae & Pope's method requires 196 HP. The power input to the tunnel is $300 \times \text{fan efficiency} (.85^2) = 217 \text{ HP}$.

The description of the computer program LOSS is presented in Appendix D.

TABLE VI
LOSS FOR EACH SECTION OF TUNNEL AT VO=200 KNOTS

SEC	Re $\times 10^{-6}$	λ	Ko	%Loss
1 test	8.88	0.0082	0.0151	10.99
2 cyl	5.16	0.0090	0.0013	0.95
3 cyl	2.90	0.0100	0.0001	0.04
4 cyl	3.04	0.0100	0.0001	0.05
5 dif	8.77	0.0083	0.0055	3.99
6 dif	8.07	0.0084	0.0253	18.42
7 dif	6.65	0.0090	0.0375	27.25
8 dif	5.29	0.0090	0.0201	14.59
9 dif	5.06	0.0090	0.0017	1.21
10 dif	4.62	0.0091	0.0019	1.39
11 dif	3.37	0.0100	0.0035	2.58
12 con	4.53	0.0091	0.0067	4.86
13 spi			0.0008	0.60
14 cor	4.56		0.0067	4.88
15 cor	4.86		0.0092	6.70
16 cor	2.77		0.0009	0.69
17 cor	2.90		0.0011	0.82

TABLE VII
TUNNEL LOSS BY THREE METHODS

VELOCITY	TOTAL LOSSES		
VELOCITY (KNOTS)	LOSS(B+P) (HP)	LOSS(R+P) (HP)	LOSS(P+H) (HP)
100.0	22.2610	25.4376	31.2752
120.0	38.0835	43.5826	53.7830
140.0	60.1842	68.9301	85.2725
160.0	89.2441	102.3171	126.8912
180.0	125.2569	143.8930	179.1000
200.0	170.4057	195.9971	244.5512

III. BLADE PERFORMANCE

A. INTRODUCTION

The "academic" wind tunnel has two stage counter - rotating fans, each fed by an electric motor of 150 hp and with a fixed speed of 1200 rpm. The main steps used in the design procedure were found in the Larson report [Ref. 4,] which contains the original blade design. The equations and the assumptions made during the design indicate that three dimensional effects were not accounted for. For this reason the method given by Borst, which is based on the blade element approach and cascade theory for determining these three dimensional effects, will be used to predict the performance of the blades. Usefully, this method requires data of two dimensional airfoils only, in order to determine the force on each section of the blade.

So, the blade system with all assumptions made during the design, (see section B - Larson report), and the Borst method, (see section C), are the material necessary to evaluate the performance of the fans. Knowing the lift developed at each blade station (eqn. 3.11) one can find the torque (eqn. 3.12) at each station. A blade station is defined non-dimensionally by the ratio of the radius of that station to the blade tip radius; the root station for this tunnel is at .267 and the tip station is at unity. Then adding the torques at all stations, and multiplying by the rotational speed, one gets the power for the blade.

B. THE LARSON REPORT

This report describes the procedure that was followed to design the blades, together with the assumptions made during the calculations.

The most important assumptions were:

- 85% fan efficiency for each stage.

- Axial velocity distribution of the flow entering the first stage fan is

$$C_m = .12 C_{mr} (rt-r) + C_{mt} , \quad (\text{eqn 3.1})$$

where C_{mr} = axial velocity at blade root,

C_{mt} = axial velocity at blade tip,

rt = tip radius,

r = local radius.

- Maximum test section velocity equal to 200 knots.

- Design lift coefficient equal to 0.64, leading to the requirement that $C_l = .8$.

- Airfoil type NACA 16 - X12 .

This design was based on forced vortex flow, in other words, the difference in static pressure across the vortex is equal to the difference in tangential velocity (dynamic) pressure. This leads us to the loading parameter (solidity x lift coefficient) and the mean velocity angle, as one can see in Appendix A, whose equations are:

$$\sigma C_l = (2(A-B)C) / (1 + (C_d/C_l) D , \text{ and} \quad (\text{eqn 3.2})$$

$$\beta_m = (\beta_1 + \beta_2) / 2 , \text{ where} \quad (\text{eqn 3.3})$$

$$A = \tan \beta_1 ,$$

$$B = \tan \beta_2 ,$$

$$C = \cos \beta_m ,$$

$$D = \tan \beta_m .$$

Using these equations and the assumptions mentioned above, the dimensions of the blades were calculated, and are given on the drawing of the blades (Ref. 9). The blades were divided into 11 (eleven) stations from root to tip; for each station the chord, thickness, leading edge angle, etc...

were determined.

C. THE BORST METHOD

This method is based on the blade element approach and the vortex theory for determining the three-dimensional effects, so that two-dimensional airfoil data can be used for determining the resultant force on each blade element. By the momentum flow theory, Borst obtained the loading parameter (solidity x lift coefficient), as a function of the angles β_1 , β_2 and β_m , that are dependent upon an induced angle of attack (α_i) at values of constant inflow angle.

The loading parameter is:

$$\sigma Cl = (2 A^2 B (C - D)) / E, \quad (\text{eqn 3.4})$$

where

- A = $\cos\beta_m$,
- B = $\cos\gamma$,
- C = $\tan\beta_1$,
- D = $\tan\beta_2$,
- E = $\cos(\beta_m - \gamma)$,
- Cl = lift coefficient,
- Cd = drag coefficient,
- β_1 = apparent inlet angle,
- β_2 = apparent outlet angle,
- β_m = angle of the mean velocity vector,
- γ = $\text{atan}(Cd/Cl)$,
- σ = solidity.

Now, based on the equations

$$\alpha_i = (\beta_1 - \beta_2) / 2, \quad \text{and} \quad (\text{eqn 3.5})$$

$$\beta_m = \beta_1 - \alpha_i, \quad (\text{eqn 3.6})$$

and the two dimensional airfoil data and design parameters for the blade, one can iterate the equation 3.4 and get the induced angle of attack for a specified test section velocity and blade station.

The angle of attack of the blade at any given station is:

$$\alpha = \beta_1 - \beta + \theta \quad , \quad (\text{eqn 3.7})$$

where β = stagger angle (Ref. 9, Ref. 4 , p.7), which is the angle between the chord line of the blade station and the line parallel to the axis of rotation of blades. (see fig. 3.1) and

θ = pitch angle (adjustable).

The Figure 3.1 shows the relation between the variables given above.

D. TORQUE AND POWER EVALUATION

We will use the Borst method (Ref. 1), to get the induced angle for correction of the two dimensional angle of attack, and the Larson Report (Ref.4) to obtain all the dimensions of the blades and the preliminary design conditions.

With this material, we are able to follow the procedure outlined below to get to the value of torque and power for each fan stage. This procedure will lead us to all velocities and angles of each blade, finalizing with the value of the torque on each blade section. After that, we evaluate the torque for the whole blade, and finally the torque and power for the fan stage.

PROCEDURE FOR EVALUATION OF TORQUE AND POWER

STEP 1) From eqn.3.1 for a given test section velocity and $n = 1,200$ rpm, calculate $W_1 = (C_m^2 + U^2)^{1/2}$,

where $U = 2\pi r n$.

As one can see, $W_1 = f(r, V_o)$ since $C_m = f(r, V_o)$. In Appendix A the axial flow velocity (C_m) was developed as

lift and drag coefficient for each section are available at MACH number $M = Wl / a$, where a = sound velocity at temperature of 100 degrees Fahrenheit, and for the design lift coefficient of 0.64, which was assumed by Larson (Ref. 4 ,p.5,6). The angle of attack used to enter the C_l vs α curve is found from eqn.3.7. Find C_l , C_d and evaluate $\gamma = \arctan(C_d/C_l)$.

STEP 5) Assuming an initial value of induced angle, evaluate the angles given by equations 3.5 and 3.6.

STEP 6) Evaluate the right side of equation 3.4 using the values found in steps 1,2, and 5; evaluate the left side of equation 3.4 using the values found in steps 3 and 4. If both sides are equal, the value of induced angle assumed is correct, otherwise, iterate.

STEP 7) The corrected angle of attack, found by using the induced angle, is seen in figure 3.1 and evaluated as follows:

$$\alpha_{cr} = \alpha - \alpha_i \quad (\text{eqn 3.9})$$

STEP 8) With corrected angle of attack, recalculate the step 4 above and get the corrected lift and drag coefficient, and evaluate γ with these values.

STEP 9) The mean velocity vector and the lift for each blade station are evaluated using the following equations:

$$W_m = C_m / \cos \beta_m \quad (\text{eqn 3.10})$$

$$L_i = 1/2 \rho W_m^2 C_l c \quad (\text{eqn 3.11})$$

where L_i = lift at blade station i per unit length,
 C_l = lift coefficient at blade station,
 W_m = mean velocity vector at blade station,
 c = chord at blade station.

STEP 10) By definition, the lift force is perpendicular to W_m . For evaluation of the torque it is necessary to get the component of the resultant force in the plane of the fan, as shown in figure 3.2. Then,

$$R_i = L_i / \cos \gamma,$$

$$F_i = R_i \cos (\beta_m - \gamma),$$

where $\gamma = \arctan (C_d/C_l)$. With C_d and C_l corrected and evaluated at step 8), and L_i, R_i, F_i are respectively the lift force, the resultant force of the lift and drag, and the force in the plane of the fan.

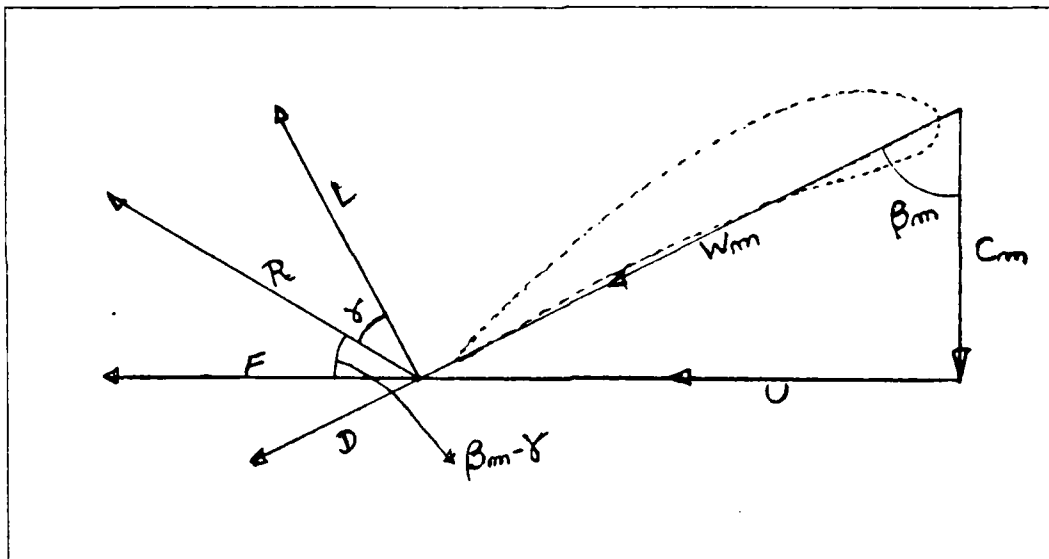


Figure 3.2 Lift Developed at Each Blade Station.

STEP 11) The force per unit length, F_i , averaged between the value at one radial station and next, times the difference in radius between these stations, is the force used for torque evaluation. This force times the mean radius of these two stations is the torque. At this point it is necessary to go through step 1 to 10 again, in order to get F_i for the next station. Then the torque on a blade section between two consecutive stations is:

$$T_i = (F_{i+1} + F_i) S R / 2 , \quad (\text{eqn 3.12})$$

where $S = (r_{i+1} - r_i)$ length between stations,

$$R = (r_{i+1} + r_i)/2,$$

and i refers to the i^{th} blade station.

STEP 12) Adding the section torques along the blade, multiplying the result by the number of blades and by the rotational speed, the power required is found. This power provides the test section velocity which was specified at the beginning of the procedure.

E. INTERACTION BETWEEN STAGES

For evaluating the torque and power for the second stage, the procedure given in the previous section can be used, but with some adjustments for the different geometric characteristics of the blade; for example, the chord, stagger angle, etc. . The tangential velocity used is the tangential velocity of the blade at the given station plus the tangential velocity of the outflow of the first stage at that station. It should be noted that the axial inflow velocity is assumed the same as for the first stage. In figure 3.4 this interaction can be seen.

The second stage should be able to accept the tangential velocity introduced in the flow by the first stage and add the same amount of power as added by the first stage. The flow leaving the second stage then has no rotation.

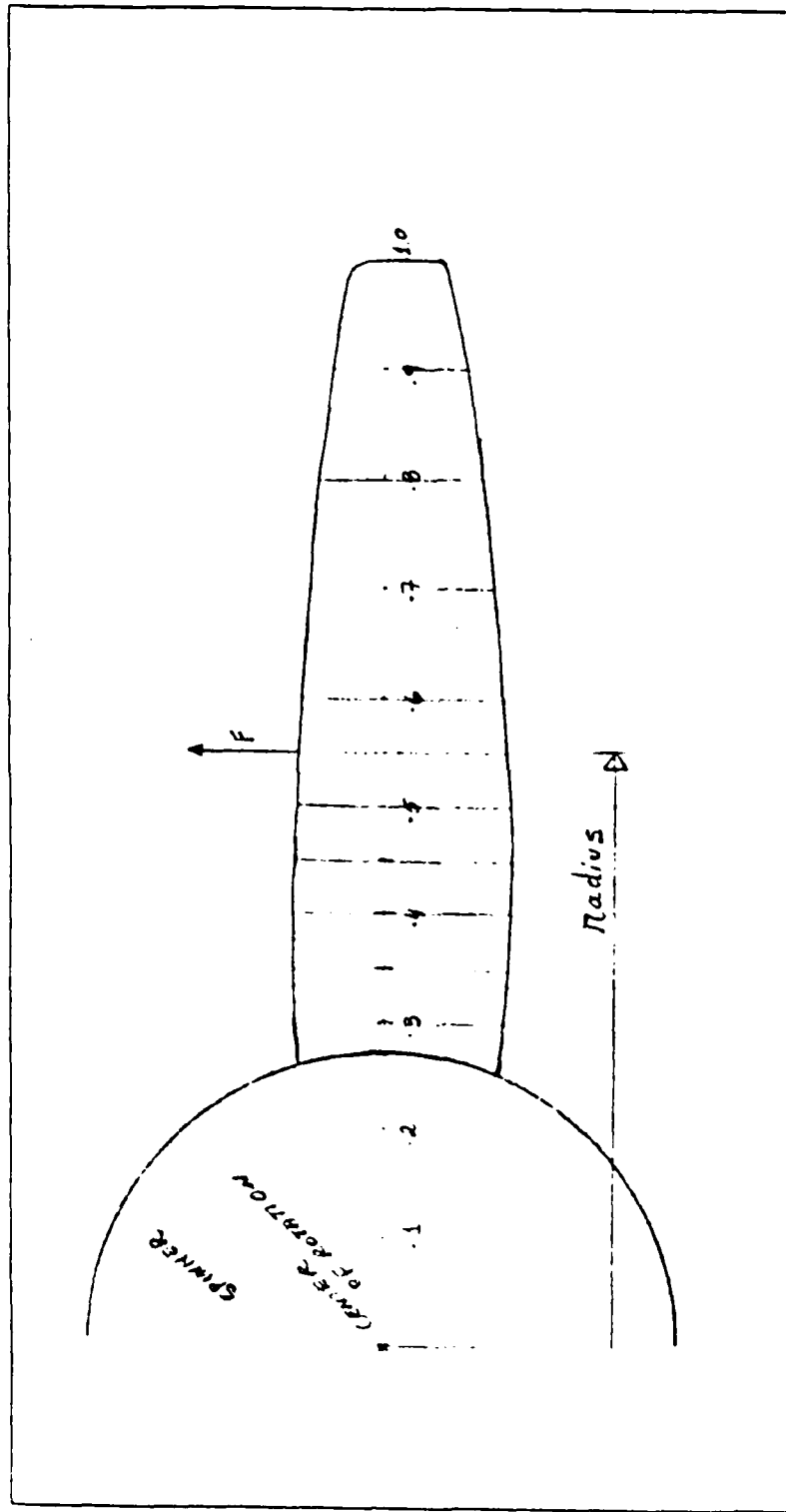


Figure 3.3 Sketch for Torque Evaluation at Each Station.

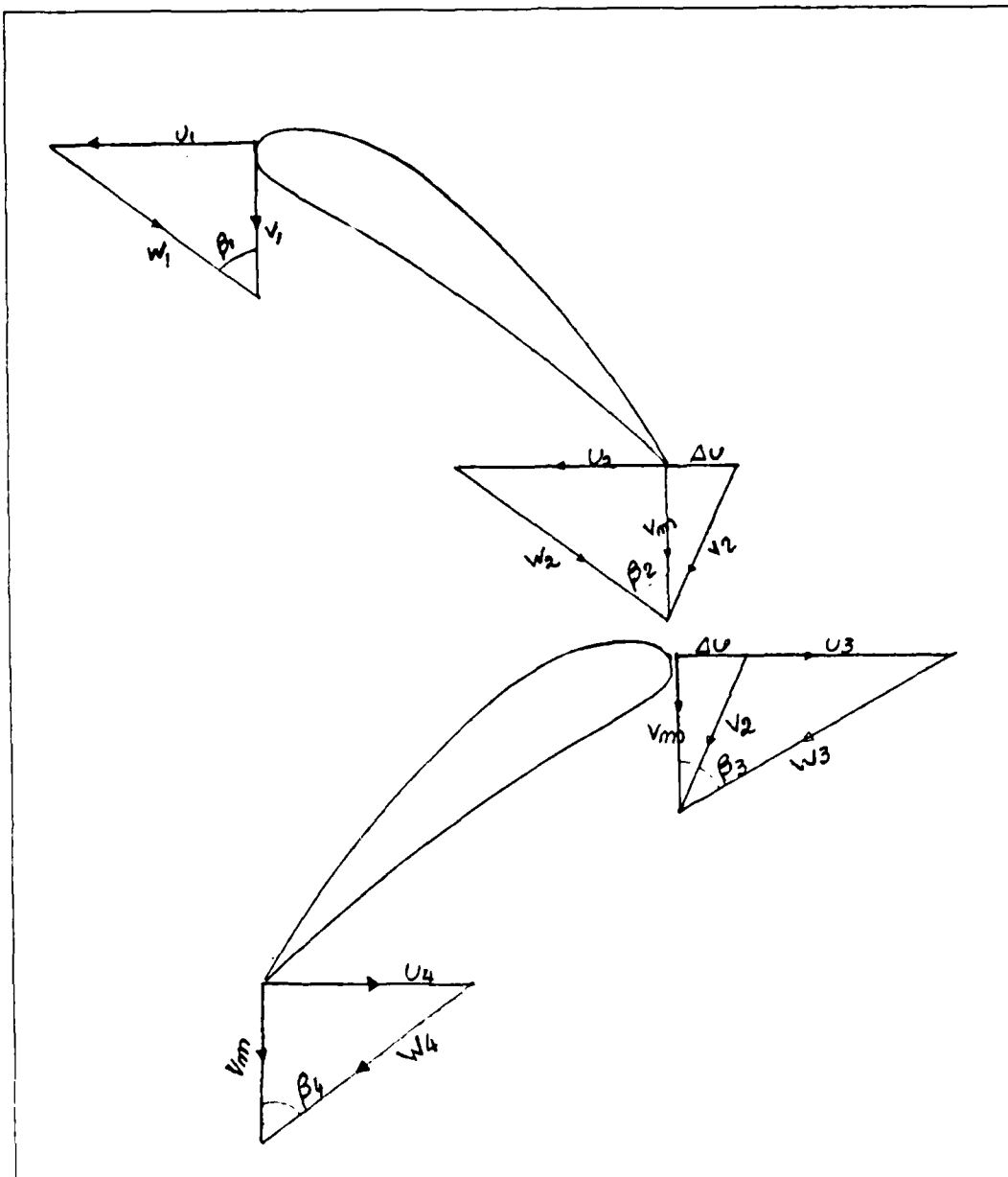


Figure 3.4 Axial Flow Velocity Triangles.

F. CONCLUSION

Using the computer program BORST and the procedure discussed in this chapter, Tables VIII through XX were obtained. For all these tables, a pitch angle of 2.4 degrees was used.

The Table VIII shows the values of the velocities from root to tip, for $V_0 = 200$ Knots, of the first fan stage. These velocities are defined as follows:

U = tangential blade velocity (ft/sec),

C_m = axial flow velocity (ft/sec),

W_1 = apparent flow velocity (ft/sec).

The chord at each station is given in feet.

The Table IX shows the Reynolds and Mach numbers at each station, for the first fan stage and at $V_0 = 200$ Knots. It is clear that compressibility effects appear at the outer 20% of the blade only. The maximum Mach number was less than .45 and the values of C_l vs α and C_l vs C_d were obtained by linear interpolation between the graphs for $M = .3$ and $M = .45$.

The Table X shows the angles between the axial flow velocity vector and the velocities relative to the blade, the stagger angle, the induced angle, the angle of attack, and the lift and drag coefficients. These values are for the first fan stage, at each station and at $V_0 = 200$ Knots. The values of lift coefficient, are distributed along the stations of the blade from .662 to .896, around the uniform value of .8, assumed by Larson. These variables are defined in Figures 3.1, 3.4, and the angles are given in degrees. As expected, at the root, the induced angle is the largest, because the greatest interference between the blades occurs there.

The Table XI shows the angle of attack, lift and drag coefficients, all with correction for the induced angle. Also shown are the lift, the resultant force and the torque. This Table refers to each station of the first fan stage,

with $V_o = 200$ Knots. The values of corrected C_l (CLCR) are distributed along the blade from .358 to .709, differently from that assumed by Larson, which was a uniform .8 .

The variables in Table XI are defined as follow:

ALPCR = corrected angle of attack (degrees),

CLCR = corrected lift coefficient,

CDCR = corrected drag coefficient,

DELL = lift force per unit length (lbf/ft),

DELF = tangential force per unit length (lbf/ft),

DTOR = torque at middle of two stations (lbf-ft).

The Tables XII, XIII and XIV, apply to the second fan stage. The variables have the same definitions as for the first stage. The Table XII shows the inflow velocity relative to the blade (W_3) larger than W_1 . This is due to the tangential flow velocity, which has a finite value after the first fan stage. At the root the difference between W_3 and W_1 is larger than at the tip, this means that the tangential flow velocity at the root is larger than at the tip. The Table XIII shows the Mach number less than .45, and the interpolation described above was again used. The Table XIV shows the C_l varying around .8, that is, from .875 to .710 as for the first fan stage.

The Table XV refers to the second stage, with the same variables as Table XI plus the variable BETA1-BETA4. This Table shows the difference between BETA1 and BETA4, which is around zero. This means that the flow after the second fan stage has no tangential velocity.

The Tables XVI and XVII, are for the uncorrected values of the angle of attack, for first stage at $V_o = 200$ Knots. The Table XVI shows the values of C_l around .8 . The Table XVII shows values of torque (DTOR) larger than those with the corrected angle of attack (Table XI).

The Tables XVIII, XIX and XX are for the second fan stage without correction of the angle of attack. A comparison of the velocities W_3 from Table XVIII, and W_3

from Table XII shows that the difference, due to the correction of the angle of attack has affected the outflow of first fan stage. The Table XIX shows the variation of BETA3 as a result of the variation of W3, just mentioned above. The variation of Cl was not so large as to affect the value of Cd. A comparison of Tables XV and XX shows that the interference between the blades reduces the torque by about 1/3 at the root and very little at the tip. This is further discussed below.

In order to visualize the effects of the correction on the angle of attack, two graphs, each with four curves, were plotted; these are:

- 1 Figure 3.5; the tangential force on the blade is shown for each station, at a specified test section velocity of 200 Knots and at a pitch angle of 2.4 degrees. The curves are referred to the first and second stages of the blades, with and without correction of the angle of attack. This figure shows again the effects of the interference. The tangential forces have the largest difference at the root, and are practically equal at the tip. The data were taken from Tables XI , XV , XVII and XX .
- 2 Figure 3.6; the angle of attack is shown for each station of the blade, at a specified test section velocity of 200 Knots and at a pitch angle of 2.4 degrees. The corrected angle of attack at the root became negative and, at the tip, that angle is practically equal to the uncorrected one. This again shows the strong effects of interference at the blade root. The curves are referred as above, and the data were taken from Tables X , XI , XIV and XV .

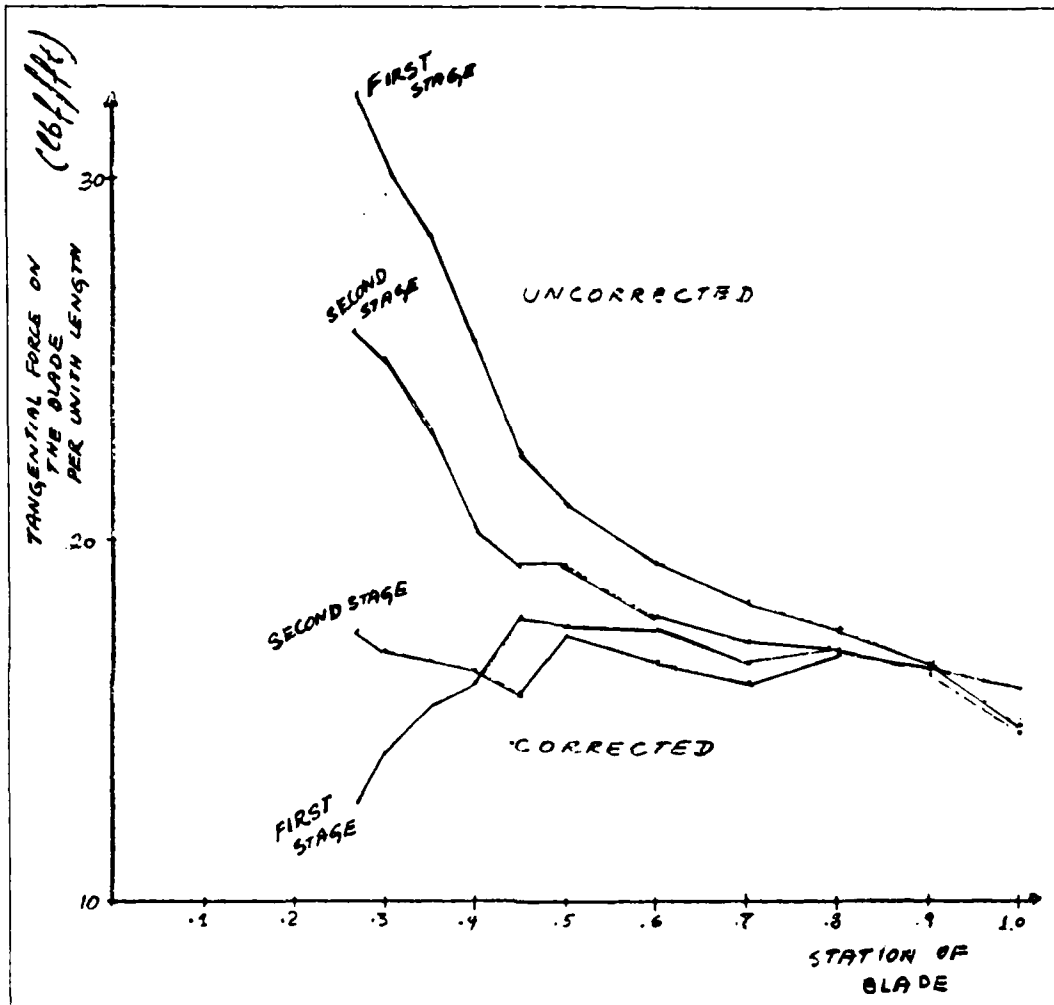


Figure 3.5 Tangential Force on the Blade at Each Station
 $V_0=200$ Knots, Pitch Angle= 2.4 degrees.

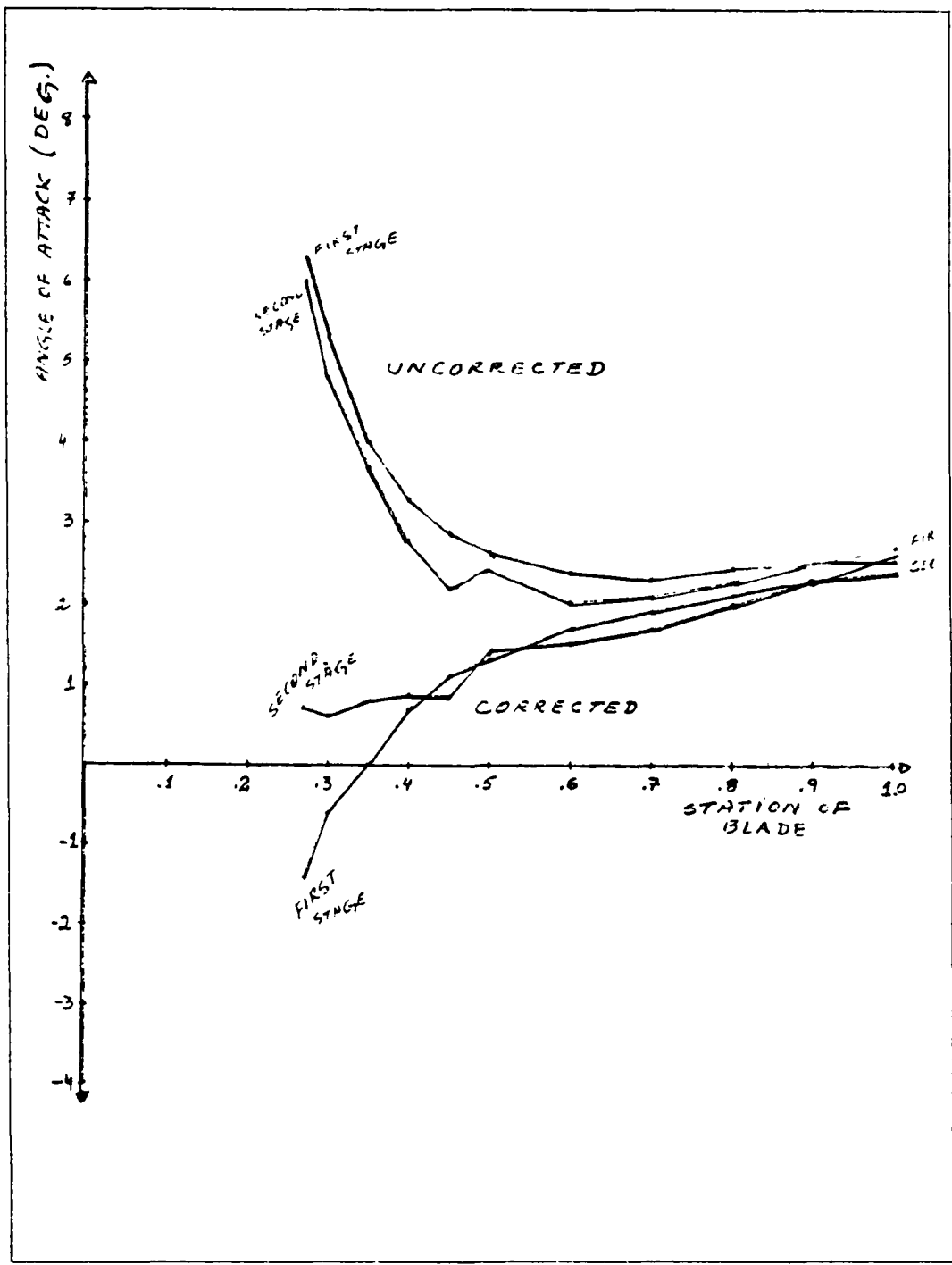


Figure 3.6 Corrected and Uncorrected Angle of Attack
 $V_0=200$ Knots, Pitch Angle= 2.4 degrees.

TABLE VIII
 VELOCITIES AT EACH STATION,
 FIRST STAGE, $V_0=200$ KNOTS

STATION	CHORD	U	CM	W1
0.267	1.112	125.821	152.606	197.787
0.300	1.049	141.372	150.340	206.369
0.350	0.958	164.934	146.907	220.873
0.400	0.875	188.496	143.475	236.887
0.450	0.802	212.058	140.042	254.126
0.500	0.738	235.620	136.609	272.357
0.600	0.631	282.744	129.743	311.090
0.700	0.546	329.868	122.877	352.010
0.800	0.481	376.992	116.011	394.438
0.900	0.422	424.116	109.145	437.935
1.000	0.344	471.240	102.279	482.212

TABLE IX
REYNOLDS AND MACH NUMBERS AT EACH BLADE STATION,
FIRST STAGE, VO=200 KNOTS

STATION	REY	MACH
0.267	1324694.000	0.171
0.300	1303483.000	0.178
0.350	1274545.000	0.190
0.400	1249081.000	0.204
0.450	1227461.000	0.219
0.500	1210513.000	0.235
0.600	1181581.000	0.268
0.700	1158453.000	0.303
0.800	1143157.000	0.340
0.900	1112776.000	0.378
1.000	998700.900	0.416

TABLE X
 ANGLES AT EACH STATION, FIRST STAGE,
 VO=200 KNOTS

THE PITCH ANGLE IS = 2.40 DEGREES POWER= 98.06 hp

STATION	BETA1	BETA2	BETAM	STAG	ALPHA1	ALPHA	CL	CD
0.267	39.505	24.124	31.814	35.580	7.691	6.325	0.896	0.015
0.300	43.239	31.538	37.388	40.370	5.850	5.269	0.863	0.015
0.350	48.308	40.301	44.305	46.670	4.004	4.038	0.832	0.015
0.400	52.723	47.360	50.042	51.770	2.682	3.353	0.774	0.012
0.450	56.559	52.981	54.770	56.030	1.789	2.929	0.701	0.012
0.500	59.895	57.299	58.597	59.650	1.298	2.645	0.681	0.009
0.600	65.351	63.854	64.602	65.330	0.749	2.421	0.664	0.009
0.700	69.569	68.641	69.105	69.590	0.464	2.379	0.662	0.009
0.800	72.895	72.277	72.586	72.850	0.309	2.445	0.678	0.009
0.900	75.568	75.148	75.358	75.420	0.210	2.548	0.696	0.009
1.000	77.754	77.479	77.617	77.450	0.137	2.704	0.718	0.011

TABLE XI
 CORRECTED LIFT AND DRAG COEFFICIENT
 LIFT AND TORQUE, FIRST STAGE, VO= 200 KNOTS

STATION	ALPCR	CLCR	CDCR	DELL	DELF	DTOR
0.267	-1.366	0.358	0.011	14.776	12.796	1.770
0.300	-0.582	0.404	0.010	17.446	14.117	3.375
0.350	0.034	0.455	0.010	21.102	15.418	4.145
0.400	0.672	0.485	0.010	24.362	16.022	5.059
0.450	1.140	0.556	0.009	30.194	17.839	5.919
0.500	1.347	0.564	0.009	32.887	17.608	13.409
0.600	1.672	0.580	0.009	38.465	17.066	15.323
0.700	1.915	0.594	0.009	44.303	16.461	17.670
0.800	2.136	0.657	0.009	54.587	17.046	19.956
0.900	2.338	0.681	0.009	61.626	16.344	20.675
1.000	2.567	0.709	0.011	63.756	14.608	

TABLE XII
 VELOCITIES AT EACH STATION,
 SECOND STAGE, VO=200 KNOTS

STATION	CHORD	U	CM	W3
0.267	0.931	125.821	152.606	238.513
0.300	0.893	141.372	150.340	242.660
0.350	0.834	164.934	146.907	252.430
0.400	0.777	188.496	143.475	263.640
0.450	0.724	212.058	140.042	276.489
0.500	0.673	235.620	136.609	292.340
0.600	0.590	282.744	129.743	327.947
0.700	0.519	329.868	122.877	366.731
0.800	0.461	376.992	116.011	407.820
0.900	0.411	424.116	109.145	450.087
1.000	0.373	471.240	102.279	492.649

TABLE XIII
REYNOLDS AND MACH NUMBER AT EACH STATION,
SECOND STAGE, $V_0 = 200$ KNOIS

STATION	REY	MACH
0.267	1337683.000	0.206
0.300	1305394.000	0.209
0.350	1268230.000	0.218
0.400	1234027.000	0.227
0.450	1205890.000	0.238
0.500	1185210.000	0.252
0.600	1165001.000	0.283
0.700	1146586.000	0.316
0.800	1132560.000	0.352
0.900	1114371.000	0.388
1.000	1106976.000	0.425

TABLE XIV
 ANGLES AT EACH STATION,
 SECOND FAN STAGE, VO=200 KNOTS

STATION	BETA3	BETA4	BETA2	STAG2	ALPHA1	ALPHA	CI	Cd
0.267	50.221	39.653	44.937	35.580	5.284	6.011	0.875	0.015
0.300	51.716	43.278	47.497	40.370	4.219	4.836	0.854	0.015
0.350	54.410	48.596	51.503	46.670	2.907	3.710	0.795	0.012
0.400	57.030	53.226	55.128	51.770	1.902	2.820	0.693	0.009
0.450	59.569	56.834	58.201	56.030	1.368	2.209	0.650	0.009
0.500	62.141	59.980	61.061	59.650	1.080	2.451	0.667	0.009
0.600	66.695	65.412	66.054	65.330	0.641	2.075	0.641	0.009
0.700	70.424	69.595	70.009	69.590	0.414	2.104	0.648	0.009
0.800	73.473	72.906	73.189	72.850	0.284	2.293	0.671	0.009
0.900	75.966	75.567	75.766	75.420	0.199	2.506	0.696	0.009
1.000	78.017	77.728	77.873	77.450	0.145	2.537	0.710	0.011

TABLE XV
 CORRECTED LIFT AND DRAG COEFFICIENT, BETA1-BETA4, AT EACH STATION,
 SECOND STAGE, VO=200 KNOIS

STATION	ALPCR	CLCR	CDCR	DELL	BETA1-BETA4	DELF	DTOR
0.267	0.727	0.487	0.010	24.236	-0.148	17.499	2.266
0.300	0.617	0.483	0.010	24.550	-0.039	16.952	3.845
0.350	0.803	0.490	0.010	26.173	-0.288	16.700	4.357
0.400	0.918	0.494	0.010	27.802	-0.502	16.346	4.790
0.450	0.841	0.491	0.010	28.894	-0.274	15.713	5.525
0.500	1.371	0.565	0.009	34.848	-0.085	17.375	13.127
0.600	1.434	0.568	0.009	39.346	-0.061	16.571	14.931
0.700	1.689	0.585	0.009	45.091	-0.026	16.099	17.351
0.800	2.009	0.652	0.009	55.592	-0.010	16.804	19.851
0.900	2.306	0.682	0.009	63.548	0.001	16.411	21.505
1.000	2.393	0.699	0.009	71.099	0.026	15.784	

TABLE XVI
 WITHOUT CORRECTION OF ANGLE OF ATTACK, FIRST STAGE, $V_0=200$ KNOTS
 ANGLES, LIFT AND DRAG COEF. AT EACH STATION
 THE PITCH ANGLE IS = 2.40 deg. POWER= 114.590hp

STATION	BETA1	BETA2	BETAM	STAG	ALPHA	CL	CD
0.267	39.505	26.589	33.524	35.580	6.325	0.896	0.015
0.300	43.239	32.930	38.450	40.370	5.269	0.863	0.015
0.350	48.308	40.892	44.837	46.670	4.038	0.832	0.015
0.400	52.723	47.302	50.166	51.770	3.353	0.774	0.012
0.450	56.559	52.533	54.646	56.030	2.929	0.701	0.012
0.500	59.895	56.858	58.442	59.650	2.645	0.681	0.009
0.600	65.351	63.545	64.478	65.330	2.421	0.664	0.009
0.700	69.569	68.441	69.020	69.590	2.379	0.662	0.009
0.800	72.895	72.161	72.536	72.850	2.445	0.678	0.009
0.900	75.568	75.074	75.325	75.420	2.548	0.696	0.009
1.000	77.754	77.412	77.585	77.450	2.704	0.718	0.011

TABLE XVII
 LIFT, RESULTANT FORCE AND TORQUE
 WITHOUT CORRECTION OF ANGLE OF ATTACK, FIRST STAGE,
 VO= 200 KNOTS

STATION	DELL	DELF	DTOR
0.267	38.400	32.367	4.133
0.300	38.362	30.458	6.722
0.350	39.314	28.378	7.101
0.400	39.065	25.482	7.157
0.450	37.845	22.419	7.257
0.500	39.339	21.039	15.625
0.600	43.683	19.364	17.160
0.700	49.020	18.182	18.831
0.800	56.050	17.527	20.424
0.900	62.698	16.647	20.975
1.000	64.297	14.754	

TABLE XVIII
 VELOCITIES AT EACH STATION
 WITHOUT CORRECTION OF ANGLE OF ATTACK, SECOND STAGE,
 VO=200 KNOTS

STATION	CHORD	U	CM	W3
0.267	0.931	125.821	152.606	232.389
0.300	0.893	141.372	150.340	238.673
0.350	0.834	164.934	146.907	250.296
0.400	0.777	188.496	143.475	263.904
0.450	0.724	212.058	140.042	279.073
0.500	0.673	235.620	136.609	295.493
0.600	0.590	282.744	129.743	331.213
0.700	0.519	329.868	122.877	369.740
0.800	0.461	376.992	116.011	410.238
0.900	0.411	424.116	109.145	452.155
1.000	0.373	471.240	102.279	495.121

TABLE XIX
 ANGLES, LIFT AND DRAG COEFF. AT EACH STATION
 WITHOUT CORRECTION OF ANGLE OF ATTACK, SECOND STAGE, $V_0=200$ KNOTS

K=	1	THE PITCH ANGLE IS =	2.40	POWER=	106.846		
STATION	BETA3	BETA4	BETAM2	STAG2	ALPHA	CL	CD
0.267	48.952	26.589	33.524	35.580	4.742	0.852	0.015
0.300	50.957	32.930	38.450	40.370	4.077	0.833	0.015
0.350	54.060	40.892	44.837	46.670	3.360	0.774	0.012
0.400	57.067	47.302	50.166	51.770	2.857	0.696	0.009
0.450	59.880	52.533	54.646	56.030	2.520	0.671	0.009
0.500	62.464	56.858	58.442	59.650	2.774	0.690	0.009
0.600	66.938	63.545	64.478	65.330	2.318	0.657	0.009
0.700	70.589	68.441	69.020	69.590	2.269	0.659	0.009
0.800	73.573	72.161	72.536	72.850	2.393	0.678	0.009
0.900	76.031	75.074	75.325	75.420	2.571	0.702	0.011
1.000	78.078	77.412	77.585	77.450	2.598	0.714	0.011

TABLE XX
 LIFT, RESULTANT FORCE AND TORQUE, SECOND STAGE
 WITHOUT CORRECTION OF ANGLE OF ATTACK, VO=200 KNOTS

STATION	DELL	DELF	DTOR
0.267	30.579	25.789	3.345
0.300	31.541	25.055	5.484
0.350	31.865	22.939	5.699
0.400	31.182	20.289	5.917
0.450	32.748	19.313	6.472
0.500	36.370	19.446	14.450
0.600	40.413	17.920	16.046
0.700	46.350	17.190	17.923
0.800	53.734	16.797	19.912
0.900	61.554	16.520	21.663
1.000	69.362	15.911	

IV. TUNNEL PERFORMANCE

A. INTRODUCTION

The tunnel performance depends on losses through the tunnel circuit and on the fan efficiency.

The performance will be evaluated to ascertain how the loss around the tunnel circuit is related to the velocity at the test section, and if the fans can provide adequate energy to generate this test section velocity. The energy provided by the blade system depends upon the pitch angle which must be limited in order to avoid stall. The pitch angle is found for the first and the second stages and checked if the flow leaving the second stage has zero rotational velocity as required.

The tunnel performance will be shown through the operational envelope of the blade system.

B. TUNNEL LOSSES

As we have seen in CHAPTER TWO the losses of each section depend on the flow velocity, which implies that they depend upon of test section velocity

Relating the losses for each tunnel section to the test section velocity we can get the total losses as a function of this velocity, and then relate the latter to flow energy required.

Using the program LOSS with test section velocity varying from 100 to 200 Knots, by increments of 20 Knots, we get the figure 4.1 which shows the energy required (η bhp.) versus test section velocity (V_0) .

C. OPERATIONAL ENVELOPE

Following the method given in Chapter 3, we find the power required from the fans as a function of test section velocity, with a number of pitch angles of the first and second stage blades.

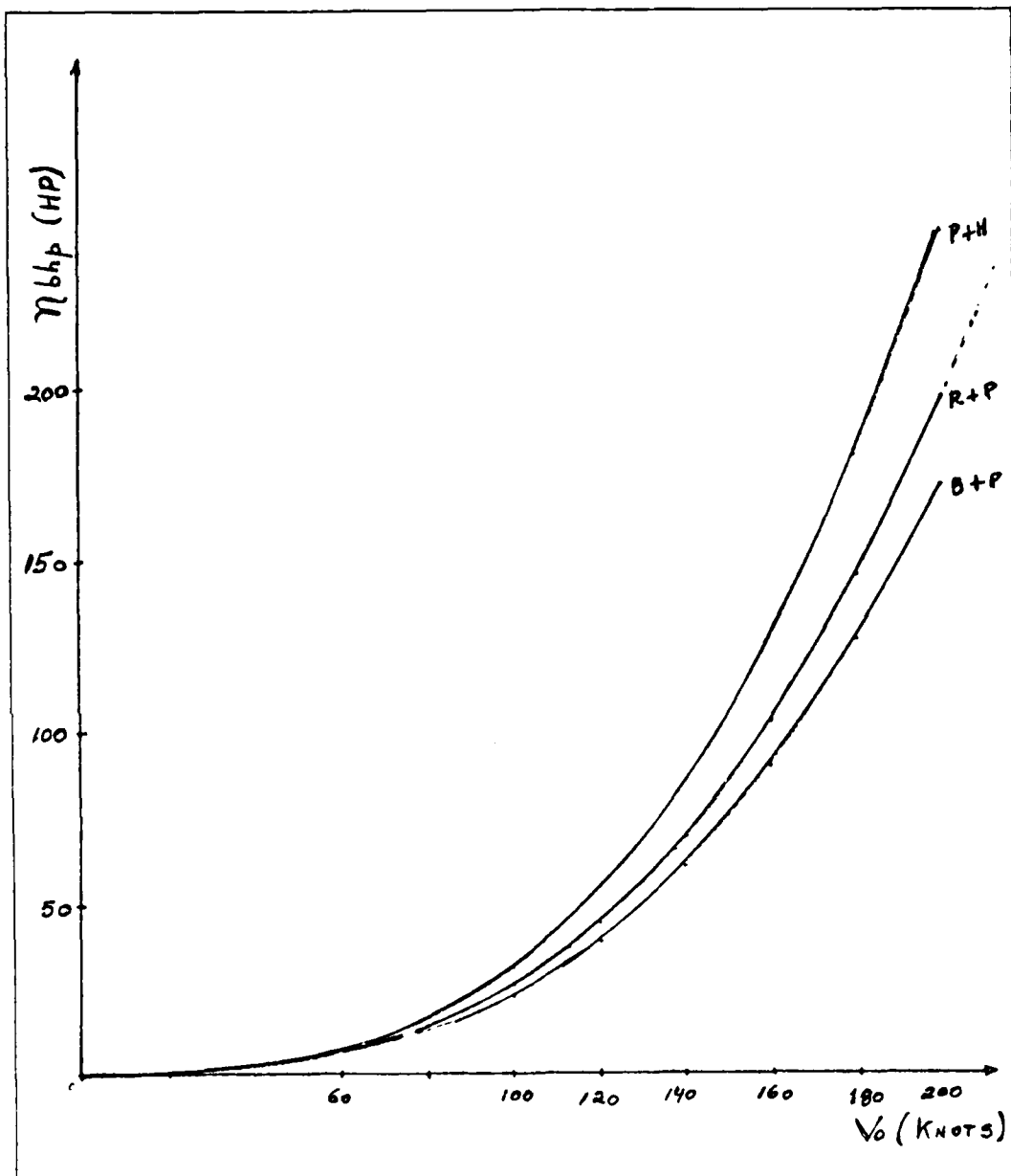


Figure 4.1 Energy Required to Overcome Tunnel Losses.

Since we know the losses around the tunnel in relation to test section velocity, we can adjust the pitch angle of blades until we get the energy coming into the flow to match the losses at same test section velocity. The program BORST was used for this.

In order to test the sensitivity of the blade flow to the approaching velocity profile, we compare the performance of the blades in uniform and skewed approach flow.

Using the axial flow velocity profile, originally used by Larson and given by equation 4.1 with the program BORST, we got the data shown in Table XXI . This Table presents the pitch angle for a specified energy and test section velocity, the maximum and minimum pitch angle at that test section velocity and its related energy. These values were plotted and are shown in Figure 4.2 . This Figure has three limit curves, root stall, tip stall and fan efficiency. The root stall curve limit is the locus of points at which, at a specified test section velocity and pitch angle, the blade stalls at the root. The tip stall curve limit is for stall at the tip. The fan efficiency curve limit is the locus where the operation of the fans is limited by the input power and the (assumed) fan efficiency, that is, $300 \text{ hp} \times .85^2 = 217 \text{ hp}$. This means that the power provided by the fan system can not exceed 217 hp approximately. The pitch angles for both stages are equal at the design speed of $V_0=200$ Knots.

Using the uniform flow velocity given by equation 4.2 , we found the data shown in Table XXII . This Table shows that the fans can operate without stall, only at a section test velocity from 160 to 180 Knots. These values were plotted in Figure 4.3 . This Figure has only the curves of root and tip stall. The fans stall before reaching the maximum power allowed by the fan efficiency. The blades of second fan stage are practically stalled at the root.

The axial velocity distribution specified for Table XXI and Table XXII are developed in Appendix A and shown below:

$$C_m = .2034 (1 - X) + .303 V_o , \text{ and} \quad (\text{eqn 4.1})$$

$$C_m = .363 V_o. \quad (\text{eqn 4.2})$$

D. FINAL CONCLUSION

The large subsonic wind tunnel at NPS, powered by two counter-rotating fans, never achieved the design specifications. The reason for the poor performance of the tunnel was unknown but believed to be due to either poorly designed fan blades or to separation in the diffuser. Being easier to analyse, the fan blades were chosen for initial study. However, to do this analysis, it was necessary to compute the losses in the whole tunnel circuit.

The results can be summarized as follows:

1) Most of the losses, about 60% of the total, was in the first diffuser. The exit end of this diffuser has a high value of divergence angle in the vertical plane, which can be the cause of a possible flow separation.

2) When the inflow velocity profile to the fans is assumed uniform, the no-stall operational envelope is substantially reduced, so there is a much greater likelihood of blade stall.

3) The variation of the pitch angle affects the performance of the fans. The pitch angles for both stages should be practically the same in order to have no flow rotation after the outlet of the second stage, provided the inflow velocity profile is the same as that assumed in the design.

4) In conclusion, although this new blade element method used to analyse the fan flow predicts some deviation from the original isolated blade analysis, it was found that the original design was adequate and, therefore, the tunnel problem is most probably due to separation in the diffuser.

TABLE XXI
OPERATIONAL ENVELOPE FOR EQUATION
4.1

V	HP	A	B	C	D	E	F
100	12.7	a	-12.3	-11.12	30.5	35.0	-
120	21.8	a	-11.13	-6.37	30.0	49.0	-
140	34.5	-8.32	-9.91	-2.09	26.0	78.0	-8.0
160	51.2	-4.75	-8.70	1.73	23.0	96.0	-4.50
180	71.9	-0.83	-7.50	5.10	15.0	128.0	-0.67
200	98.0	2.40	-6.30	8.08	27.0	150.0	2.40

Legend

V_0 - test section velocity

HP - power

A - pitch angle of first stage

B - lower limit of pitch angle

C - upper limit of pitch angle

D - lower power limit

E - upper power limit

F - pitch angle of second stage

a - the pitch angle at which the blade does not stall;

provides more power than needed.

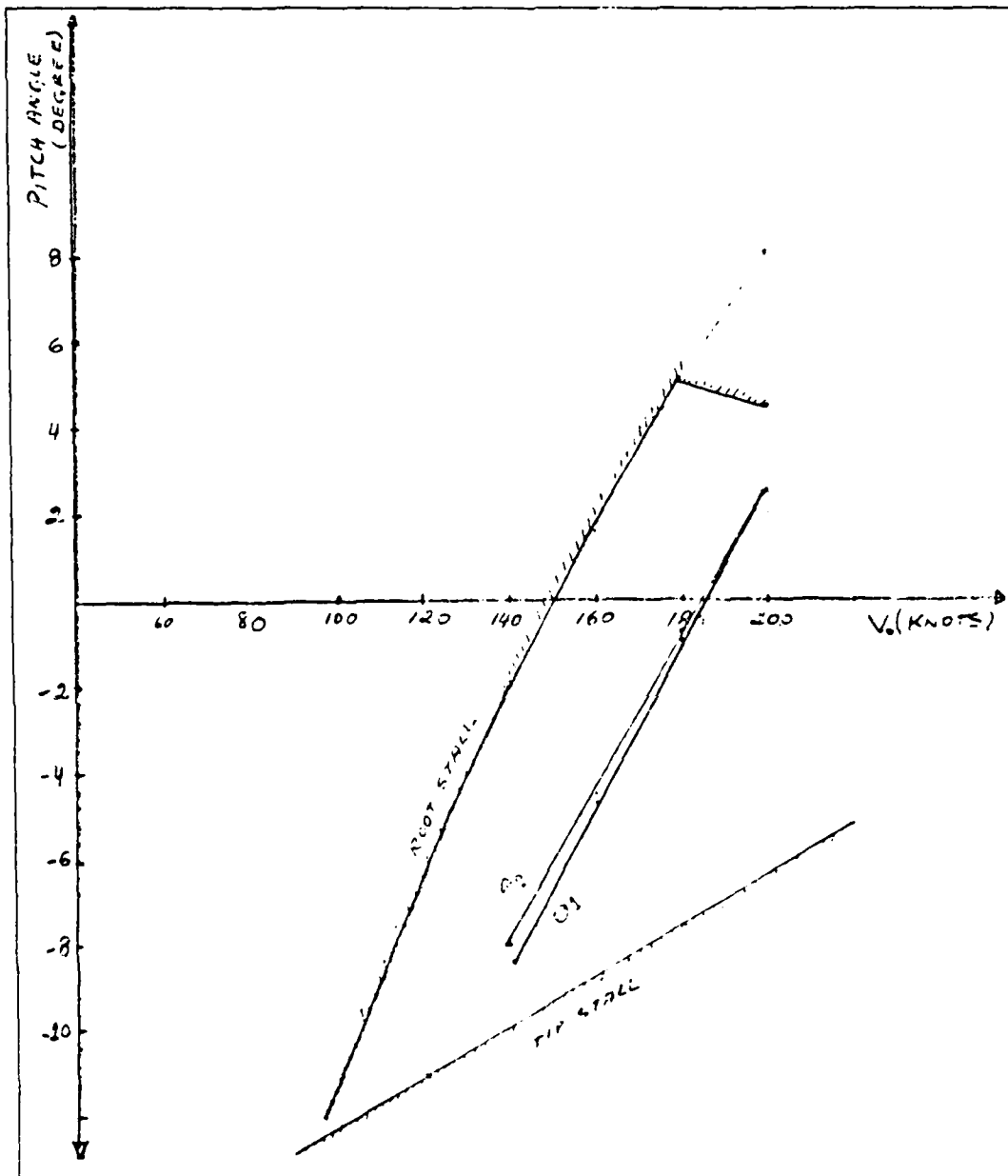


Figure 4.2 Operational Envelope for Equation 4.1.

TABLE XXII
OPERATIONAL ENVELOPE FOR EQUATION
4.2

V	HP	A	B	C	D	E	F
100	12.7	b	-	-	-	-	-
120	21.8	b	-	-	-	-	-
140	34.5	a	-8.21	-8.14	36.2	36.3	-7.74
160	51.2	-4.85	-6.80	-4.50	35.1	52.4	-4.4
180	71.9	-1.50	-5.38	-1.19	33.0	74.0	-1.25
200	98.0	c	-3.97	1.82	31.9	95.6	-

Legend

b - the blade is stalled for any pitch angle
c - the pitch angle at which the blade does not stall;
provides less power than needed

The other variables have the same meaning as in table XXI

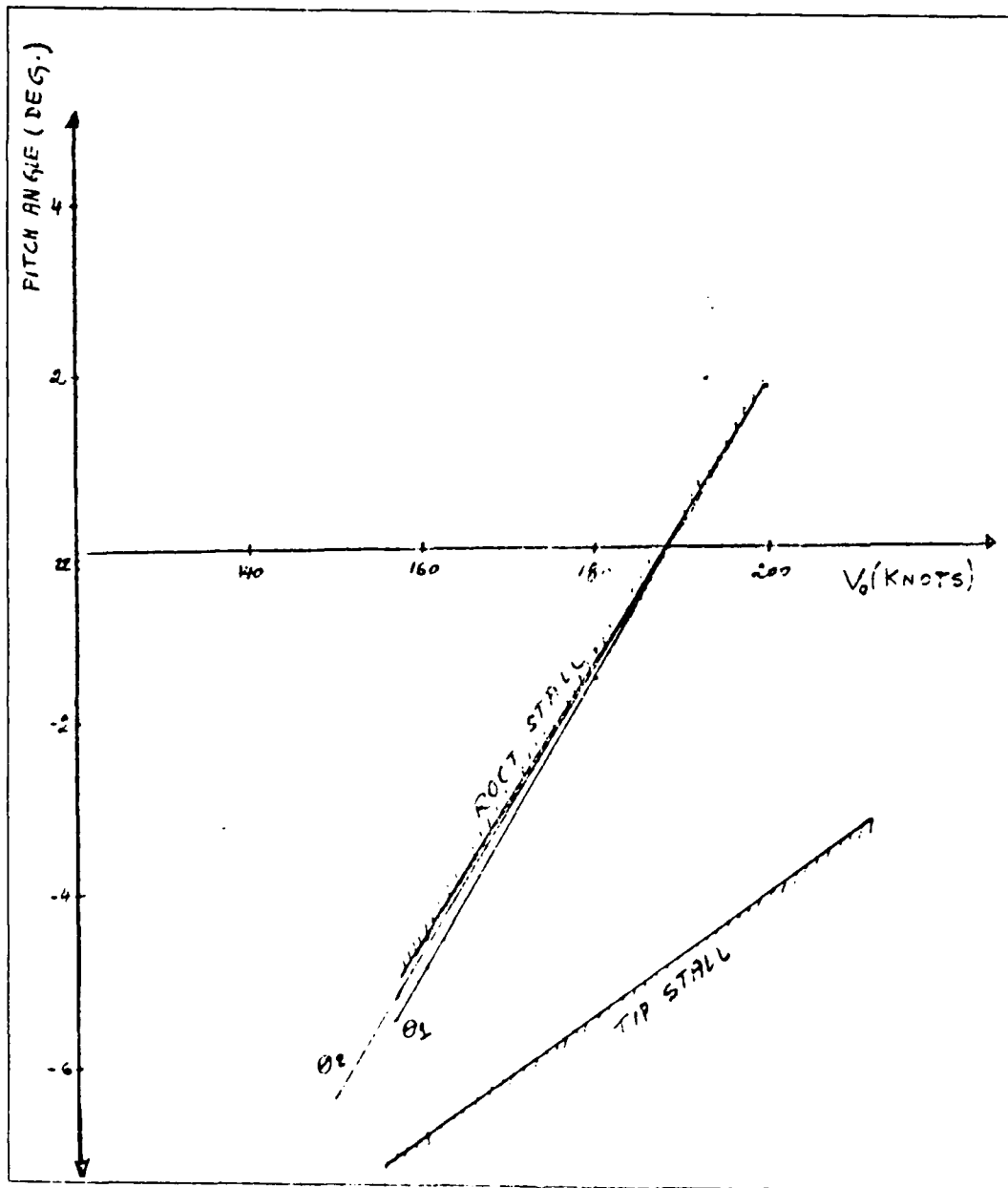


Figure 4.3 Operational Envelope for Equation 4.2.

APPENDIX A
SPECIFIED FUNCTIONAL FORMS

CORNER

The evaluation of the corner loss using the turning vane loss function presented in appendix B of reference 6 , (p.35) with the flow turning angle equal to 90 degrees, leads to the equation given by RAE & POPE [Ref. 2: p.90]. The equation for the turning vane loss coefficient is

$$KTV = -1.605670E-01 + 1.446753E-02\phi - 2.570748E-04\phi^2 + 2.066207E-06\phi^3 - 6.335764E-09\phi^4 ,$$

with $\phi = 90$ degrees is found $KTV = .15$.

The equation for turning vane loss function is
 $K = KTV (2/3 + (1/3(\log_{10} Rnr / \log_{10} Rn)^{2.58}))$,
 where

$Rnr = 500,000$ (reference Reynolds number,
 according to ref. 2 p.89),

and $\log_{10} 500,000 = 5.7$.

Substituting these values in the equation of the turning vane loss function, the equation given by Rae & Pope appears as follows:

$$K = 0.15 (2/3 + 29.7/\log_{10} Rn)^{2.58},$$

$$K = (0.1 + 4.45/(\log_{10} Rn)^{2.58}),$$

$$K_o = K (D_o/D)^4 .$$

LOADING PARAMETER (Larson)

The loading parameter used by Larson in his report comes from blade element theory, where the effects of drag are considered. This is also shown in Osborne [Ref. 11: p.147], by equation

$$Vu/Wm = 1/2 Cl (1 + Cd/Cl \cotan (\beta - \alpha)) ,$$

where β = mean blade velocity angle .

The Larson report (pp. 5,6) gives

$$\cotan (\beta - \alpha) = \tan (\beta_m),$$

and rearranging the term V_u/W_m as

$V_u/W_m = (U/C_m - (U-V_m)/C_m) C_m/W_m$, and using the axial velocity triangles, the following relations are assured:

$$U/C_m = \tan\beta_1, (U-V_u)/C_m = \tan\beta_2,$$

$$C_m/W_m = \cos\beta_m.$$

Substituting these relations into the equation given by Osborne, the final equation is

$\sigma C_l = (2(\tan\beta_1 - \tan\beta_2)\cos\beta_m)/(1 + C_d/C_l \tan\beta_m)$ and is the equation used by Larson.

AXIAL FLOW VELOCITIES.

Larson assumed in his report the axial flow velocity as:

$$C_m = .12 r_t (1 - r/r_t) + C_{mt} \quad (1)$$

where r_t = tip radius, r = station radius, C_{mt} = axial velocity at tip blade, and C_{mr} = axial velocity at the root of the blade. Integrating the product of the cross section area of the fan duct at the blades times C_m , from root to tip, and setting it equal to the product of the area times the velocity of the test section, we find:

$$14.9 V_o = 5.465 C_{mr} + 41.037 C_{mt}.$$

In the equation of C_m , when r is the radius of the blade root, $C_m = C_{mr}$, and

$$C_{mr} = C_{mt} / 0.67. \quad (2)$$

Equating (1) and (2), the axial velocity profile for our tunnel is found as:

$$C_m = (0.2034 (1 - r/r_t) + .303) V_o$$

UNIFORM AXIAL FLOW VELOCITY.

This axial profile velocity is used only for purposes of comparison. From the continuity equation $C_m = A_o V_o / A$ and, taking the known values, we find $C_m = .363 V_o$.

APPENDIX B
SAMPLE CALCULATIONS

Evaluation of the blade station torque.

For first stage

Following the 'torque and power' procedure given in chapter three, at a specified station the data are as follows:

General data:

- curves of C_l vs α and C_l vs C_d for airfoil NACA 16-X12 at $M=.3$ and $M=.45$.
- $a=1,160$ ft/sec
- $\rho = .0023$ slug/ft³
- $\nu = .000166$ ft²/sec
- $r_t = 3.75$ ft
- $C_{l_{des}} = .64$
- $V_o = 200$ Knots = 337.55 ft/sec
- $B = 4$ blades
- $\theta = 2.4$ deg.

At specified station:

- $X = .3$
- $c = 1.049$ ft
- $\beta = 40.37$ deg.

STEP 1) $C_m = (.2034(1-.3)+.303) \times 337.55 = 150.34$ ft/sec

$U = 2 \times 3.1416 \times .3 \times 3.75 \times 1200/60 = 141.37$ ft/sec

$W_1 = (150.34^2 + 141.37^2)^{1/2} = 206.37$ ft/sec

STEP 2) $\beta_1 = \arctan(141.37/150.34) = 43.24$ deg.

STEP 3) $\sigma = (4 \times 1.049) / (2 \times 3.1416 \times .3 \times 3.75) = .5936$

STEP 4) $M = 206.37/1,160 = .18$

$\alpha = 43.24 - 40.37 + 2.4 = 5.27$ deg.

Entering into curve at $M=.3$ are found $C_l=.87$ and $C_d = .015$.

$\gamma = \arctan(.015/.87) = .988$

STEP 5) assume $\alpha_i = 5.85$ deg.

$$\beta_2 = 43.24 - 2 \times 5.85 = 31.54 \text{ deg.}$$

$$\beta_m = 43.24 - 5.85 = 37.39 \text{ deg.}$$

STEP 6) right side = $((2 \times \cos^2 37.39 \times \cos .988 (\tan 43.24 - \tan 31.54)) / \cos(37.39 - .988)) =$
 $= .51225$

$$\text{left side} = .5936 \times .87 = .5164$$

The induced angle assumed is adequate and equal to $\alpha_i = 5.85$ deg.

STEP 7) $\alpha_{cr} = 5.27 - 5.85 = -.58$ deg.

STEP 8) $C_{l_{cr}} = .41$ $C_{d_{cr}} = .01$

$$\gamma_{cr} = \arctan (.01 / .41) = 1.397 \text{ deg.}$$

STEP 9) $W_m = 150.34 / \cos 37.39 = 189.22$ ft/sec

$$L_i = 1/2 \times .0023 \times 189.22^2 \times .41 \times 1.049 = 17.71 \text{ lbf/ft}$$

STEP 10) $R_i = 17.71 / \cos 1.397 = 17.71$ lbf/ft

$$F_i = 17.71 \cos(37.39 - 1.397) =$$
$$= 14.33 \text{ lbf/ft}$$

NEXT STATION

At specified station

$$X = .35$$

$$c = .958 \text{ ft}$$

$$\beta = 46.67 \text{ deg.}$$

STEP 1) $C_m = (.2034(1 - .35) + .303) \times 337.55 = 146.90$ ft/sec

$$U = 2 \times 3.1416 \times .35 \times 3.75 \times 1200 / 60 = 164.93 \text{ ft/sec}$$

$$W_1 = (146.90^2 + 164.93^2)^{1/2} = 220.86 \text{ ft/sec}$$

STEP 2) $\beta_1 = \arctan(164.93 / 146.90) = 48.31$ deg.

STEP 3) $\sigma = (4 \times .958) / (2 \times 3.1416 \times .35 \times 3.75) = .4647$

STEP 4) $M = 220.86 / 1,160 = .19$

$$\alpha = 48.31 - 46.67 + 2.4 = 4.04 \text{ deg.}$$

Entering into curve at $M = .3$ are found $C_l = .83$ and $C_d = .015$.

$$\gamma = \arctan (.015 / .83) = 1.033 \text{ deg.}$$

STEP 5) assume $\alpha_i = 4.00$ deg.

$$\beta_2 = 48.31 - 2 \times 4.00 = 40.31 \text{ deg.}$$

$$\beta_3 = 48.31 - 4.00 = 44.31 \text{ deg.}$$

STEP 6) right side = $((2 \times \cos^2 44.31 \times \cos 1.033 (\tan 48.31 - \tan 40.31)) / \cos(44.31 - 1.033)) =$
 $= .3864$

$$\text{left side} = .4647 \times .83 = .3866$$

The induced angle assumed is adequate and equal to $\alpha_i = 4.00$ deg.

STEP 7) $\alpha_{cr} = 4.04 - 4.00 = .04$ deg.

STEP 8) $C_{l_{cr}} = .455$ $C_{d_{cr}} = .01$

$$\gamma_{cr} = \arctan (.01 / .455) = 1.259 \text{ deg.}$$

STEP 9) $W_m = 146.9 / \cos 44.3 = 205.25$ ft/sec

$$L_i = 1/2 \times .0023 \times 205.25^2 \times .455 \times .958 = 21.11 \text{ lbf/ft}$$

STEP 10) $R_i = 21.11 / \cos 1.259 = 21.11$ lbf/ft

$$F_i = 21.11 \cos(44.31 - 1.259) =$$
$$= 15.43 \text{ lbf/ft}$$

For both station at $X = .3$ and $X = .35$

STEP 11) $T = (14.33 + 15.43) / 2 \times 3.75 \times .05 \times .325 \times 3.75 =$
 $= 3.40$ lbf-ft

After that, adding all station torques and multiplying by the rotational speed, the power is found.

For the second stage, the same procedure can be followed with some adjustments as mentioned before in chapter 3, section E.

APPENDIX C
DESCRIPTION OF COMPUTER PROGRAMS

The following pages contain the FORTRAN PROGRAMS developed to evaluate the blade performance and the tunnel losses.

The LOSS FORTRAN is a program to evaluate the losses around the circuit of the large Academic Wind Tunnel of NPS. This program uses one subroutine called SKIN to calculate the skin friction when the Reynolds number is given; it does this by means of equation 2.1. The main program uses the equations for K_o and Re_y for each section of the tunnel, given in chapter two. The meaning of variables used in the program are given at beginning of the main program and subroutine. The listing of the program is presented in Appendix D.

The BORST FORTRAN is a program used to evaluate the performance of the blades of both stages. This program uses the procedure presented in chapter three section D, to evaluate the torque and power of the first stage, and section E to evaluate the torque and power of the second ; it uses six subroutines as follows: FIRST is a subroutine to evaluate the parameters of the blade of each station at a specified test section velocity, for the first stage. SECOND is a subroutine like FIRST but it evaluates for the second stage. CLNEW is a subroutine to compute the lift coefficient for each section of the blade using Newton's Forward and Backward Interpolation Formula, with the data given by curves of C_l vs α in reference 12 . CDNEW is a subroutine to compute the drag coefficient for each section using the same formula as in CLNEW, with data given by the curve of C_d vs C_l in the same reference as in CLNEW. INDUC is a subroutine used to compute the induced angle of attack

through iterations using the equation 3.4. LIFT is a subroutine to compute the torque and power for second stage of blades calling all the subroutines except FIRST; this subroutine is called by the main program after it evaluates the torque and power of the first stage.

This program is listed in Appendix E and a description of parameters appears at the beginning of either the main program or the subroutine.

APPENDIX D
COMPUTER PROGRAM ' LOSS '

```

$JOB      ID,XREF,EXT
CCCCCCCCCCCC
SUBROUTINE TO COMPUTE THE SKIN FRICTION
        USAGE
        CALL SKIN (R,FRIC)
        DESCRIPTION OF PARAMETERS
        R - REYNOLDS NUMBER (INPUT)
        FRIC - SKIN FRICTION COEFFICIENT (OUTPUT)

SUBROUTINE SKIN(R,FRIC)
REAL R,FRIC,A,B,DELTA,TEMP1,TEMP
TEMP1=300.
FRIC=.006
DELTA=.001
A=SQRT(FRIC)
B=2.*ALOG10(R*A)-1./A
TEMP=ABS(B-.8)
IF (TEMP1.GT. TEMP) .LT..001) GO TO 120
FRIC=FRIC-DELTA
DELTA=DELTA/10.
IF (DELTA.LT..00000001)GO TO 120
GO TO 130
TEMP1=TEMP
FRIC=FRIC+DELTA
GO TO 110
RETURN
END

110
100
130
120

MAIN MAIN MAIN PROGRAM
        DESCRIPTION OF PARAMETERS
BRAD(K) = OVERALL ENERGY LOSSES, CORNER EVALUATED BY PANK & BRAD
CDF      = FRICTION DRAG COEFFICIENT
CDO      = DRAG COEFFICIENT
FRIC     = SKIN FRICTION COEFFICIENT
HOL (K) = OVERALL ENERGY LOSSES, CORNER EVALUATED BY PANK & HOLD
LOSS     = LOSS VECTOR (K)
PER      = PERCENTAGE OF OVERALL LOSSES FOR EACH SECTION
CCCCCCCCCCCC

```

POPE(K) = OVERALLS ENERGY LOSSES, CORNER EVALUATED BY RAE & POPE

REY = REYNOLDS NUMBER VECTOR
SUM1 = SUM OF LOSS VECTOR { CORNER BY RAE & POPE }
SUM2 = SUM OF LOSS VECTOR { CORNER BY PANK & BRAD }
SUM3 = SUM OF LOSS VECTOR { CORNER BY PANK & HOLD }
V = TEST SECTION VELOCITY (FT/SEC)
V1 = TEMPORAL VARIABLE
V2(K) = TEST SECTION VELOCITY (KNOTS)

REAL LOSS(30), REY(30), FRIC(30), V, CDF, CDO, HOL(30),
PER(30), SUM1, SUM2, SUM3, POPE(30), BRAD(30),
V2(30), V1,
INTEGER I, K
V = 168.778
K = 1
V2(K) = 100.

1
2

CCCCCCCC

CYLINDER # 1
REY(1) = 26300.*V
CALL SKIN(REY(1), FRIC(1))
LOSS(1) = 1.834*FRIC(1)

201

CC

CYLINDER # 2
REY(2) = 15300.*V
CALL SKIN(REY(2), FRIC(2))
LOSS(2) = .1448*FRIC(2)

CC

CYLINDER # 3
REY(3) = 8600.*V
CALL SKIN(REY(3), FRIC(3))
LOSS(3) = .0051*FRIC(3)

CC

CYLINDER # 4
REY(4) = 9010.*V
CALL SKIN(REY(4), FRIC(4))
LOSS(4) = .0067*FRIC(4)

CC

DIVERGENCE # 1 PART # 1
REY(5) = 26000.*V
CALL SKIN(REY(5), FRIC(5))
LOSS(5) = .5367*FRIC(5) + .00103

CC

DIVERGENCE # 1 PART # 2
REY(6) = 23900.*V
CALL SKIN(REY(6), FRIC(6))
LOSS(6) = .5416*FRIC(6) + .0208

CC

DIVERGENCE # 1 PART # 3
REY(7) = 19700.*V

CC

C C CALL SKIN(REY(7), FRIC(7)) + .0355
 C C LOSS(7) = .2232 * FRIC(7) + .0355
 C C DIVERGENCE # 1 PART # 4
 C C REY(8) = 15670 * V
 C C CALL SKIN(REY(8), FRIC(8)) + .0196
 C C LOSS(8) = .054 * FRIC(8) + .0196
 C C DIVERGENCE # 2
 C C REY(9) = 15000 * V
 C C CALL SKIN(REY(9), FRIC(9)) + .0004
 C C LOSS(9) = .1400 * FRIC(9) + .0004
 C C DIVERGENCE # 3
 C C REY(10) = 13700 * V
 C C CALL SKIN(REY(10), FRIC(10)) + .0011
 C C LOSS(10) = .09 * FRIC(10) + .0011
 C C DIVERGENCE # 4
 C C REY(11) = 10000 * V
 C C CALL SKIN(REY(11), FRIC(11)) + .003
 C C LOSS(11) = .055 * FRIC(11) + .003
 C C CORNER # 1 POPE & BRADSHAW
 C C REY(14) = 1646 * V
 C C LOSS(14) = .0069 * V + .3122 / (ALOG10(REY(14))) ** 2.58
 C C LOSS(18) = .013 * V
 C C CORNER # 2 POPE & BRADSHAW
 C C REY(15) = 1890 * V
 C C LOSS(15) = .00905 * V + .4118 / (ALOG10(REY(15))) ** 2.58
 C C LOSS(19) = .016 * V
 C C CORNER # 3 POPE & BRADSHAW
 C C REY(16) = 609.5 * V
 C C LOSS(16) = .00094 * V + 0.428 / (ALOG10(REY(16))) ** 2.58
 C C LOSS(20) = .0023 * V
 C C CORNER # 4 POPE & BRADSHAW
 C C REY(17) = 334.2 * V
 C C LOSS(17) = .00113 * V + .0515 / (ALOG10(REY(17))) ** 2.58
 C C LOSS(21) = .0032 * V
 C C CONTRACTION CONE
 C C REY(12) = 13420 * V
 C C CALL SKIN(REY(12), FRIC(12))
 C C LOSS(12) = .7338 * FRIC(12)
 C C SPINNER
 C C GDF = (.455 / (ALOG10(24500 * V))) ** 2.58 * 31.027


```

C 58      FORMAT(/, I3, 30X, 2F15.4)
C
C          RELATED TO CORNER EVALUATION BY PANKHURST & HOLDER
C
SUM3=0
DO 401 I=1, 13
SUM3=SUM3+LOSS(I)
CONTINUE
DO 402 I=22, 25
SUM3=SUM3+LOSS(I)
CONTINUE
DO 603 I=1, 13
PER(I)=LOSS(I)/SUM3*100.
CONTINUE
DO 604 I=22, 25
PER(I)=LOSS(I)/SUM3*100.
CONTINUE
HOL(K)=.000031232*V**3*SUM3/.9
WRITE(6, 467) VELOCITY, ' ', TOTAL LOSSES ', IOX, 'HP' )
FORMAT( /, 463) V2(K), SUM3, HOL(K)
WRITE(6, 463) F15.8, F15.8, ' CORNER BY HOLDER ' )
WRITE(6, 657) (I, REY(I), FRIC(I), LOSS(I), PER(I), I=1, 13)
FORMAT( /, I3, 4F15.4)
WRITE(6, 658) I, LOSS(I), PER(I), I=22, 25)
FORMAT( /, I3, 30X, 2F15.4)
V1=V2(K)
K=K+1
V2(K)=V1+20
V=V+20*6076/3600
IF(V2(K)-220) 201, 202, 202
WRITE(6, 466) (V2(K), BRAD(K), POPE(K), HOL(K), K=1, 6)
FORMAT( /, F 8.1, 3F15.8)
RETURN
END
202
466
$ENTRY

```

APPENDIX E

COMPUTER PROGRAM ' BORST '

```

$JOB
CCCCCCCCC
SUBROUTINE TO COMPUTE THE INITIAL VELOCITIES, INITIAL ANGLES,
REYNOLDS NUMBER AND MACH NUMBER FOR FIRST STAGE
DESCRIPTION OF PARAMETERS
THE PARAMETERS ARE ALL REFERRED TO BLADE SECTION, WHEN
NO SPECIFIED.
INPUT
X = POSITION OF BLADE SECTION GIVEN BY LOCAL RADIUS
  DIVIDED BY TIP RADIUS
V = TEST SECTION VELOCITY (KNOTS)
C = CHORD
ASOUND = SOUND VELOCITY AT 100 DEGREE FAHRENHEIT
VISC = KINEMATIC VISCOSITY AT 100 DEGREE FAHRENHEIT AND
  PRESSURE AT 2,246 LBF/FT2
OUTPUT
CM = AXIAL FLOW VELOCITY
CU2 = ABSOLUTE TANGENTIAL VELOCITY LEAVING
U = TANGENTIAL VELOCITY OF BLADE SECTION
BETA = APPARENT AIR FLOW ENTERING ANGLE
W1 = APPARENT AIR FLOW VELOCITY
REY = REYNOLDS NUMBER
M = MACH NUMBER
SUBROUTINE FIRST(X,V,C,ASOUND,VISC,CM,CU2,U,BETA,W1,REY,M)
REAL X,C,ASOUND,VISC,CM,CU2,U,BETA,W1,REY,M,V,V1
V1=V*6076/3600
CM=(2034*(1.0-X)+.303)*V1
CU2=363*V1
U=13.2/X
BETA=471.24*X
W1=SQRT(U**2/VISC)
REY=W1*C/ASOUND
M=RETURN
END
CCCC

```

CCCCCCCCCCCC

SUBROUTINE TO COMPUTE THE INITIAL VELOCITIES INITIAL ANGLE,
REYNOLDS NUMBER AND MACH NUMBER FOR SECOND STAGE

```

      C
      DESCRIPTION OF PARAMETERS
      ALL PARAMETERS ARE REFERRED TO SECOND STAGE AND THEY HAVE
      THE SAME MEANING OF THAT FOR THE FIRST STAGE EXCEPT
      BT= APPARENT AIR FLOW ANGLE LEAVING THE FIRST STAGE

      SUBROUTINE SECOND(X,V,C,BT,ASOUND,VISC,CM,CU2,U,BETA,W1,REY,M,BT,V,VI)
      REAL X,C,ASOUND,VISC,CM,CU2,U,BETA,W1,REY,M,BT,V,VI
      VI=V*6076/3600
      CM=(.2034*(1.0-X)+.303)*VI
      CU2=13.2/X
      U=471.24*X
      BETA=ATAN((2.*U-CM*TAN(BT))/CM)**2
      W1=SQRT((2.*C/ASOUND)**2+CM)**2
      REY=W1/ASOUND
      RETURN
      END

```

C

CCCCCCCCCCCCCCCCCCCC

SUBROUTINE TO COMPUTE LIFT AND TORQUE FOR SECOND STAGE

THIS SUBROUTINE USES THE OTHER THREE SUBROUTINES ,CLNEW,
CDNEW AND INDUC.

DESCRIPTION OF PARAMETERS

ALL PARAMETERS ARE REFERRED TO SECOND STAGE AND AT STATION
WHEN NO SPECIFIED

```

      C
      STDG = STDG2 = APPARENT INLET FLOW ANGLE (DEG.)
      STAG = STAG2 = STAGGER ANGLE (DEG.)
      PITCH= PITCH ANGLE (DEG.)
      M = SM = MACH NUMBER
      BETA = SETA = APPARENT INLET FLOW ANGLE (RAD.)
      X = LOCAL STATION OF BLADE
      C = SC = CHORD (FT)
      CM = U = AXIAL FLOW VELOCITY (FT/SEC)
      U = U = BLADE STATION TANGENTIAL VELOCITY (FT/SEC)
      RO = RO = SPECIFIC DENSITY (SLUG/FT3)

```

CCCCCCCCCCCC

DELF = DELF = FORCE PER UNIT LENGTH IN THE DIRECTION OF
 TANGENTIAL VELOCITY OF BLADE (LB/FT)
 BETAM = SETAM = MEAN AIR INFLOW ANGLE (DEG.)
 BET2 = SET2 = LEAVING ANGLE (DEG.)
 ALPHA = INDUCED ANGLE OF ATTACK (DEG.)
 ALPHA = ANGLE OF ATTACK (DEG.)
 CL = LIFT COEFFICIENT
 CD = DRAG COEFFICIENT
 ALPCR = CORRECTED ALPHA (DEG.)
 CLCR = CORRECTED CL
 CDCR = CORRECTED CD
 DELL = LIFT PER UNIT LENGTH (LB/FT)

CCCCCCCCCCCC

```

SUBROUTINE LIFT(STDG, STAG, PITCH, M, BETA, X, C, CM, U, CU2, RO, DELF,
  BETAM, BET2, ALPHA, ALPHA, CL, CD, ALPCR, CLCR, CDCR, DELL)
COMMON CL364(20), CL464(20), CD364(20), CD464(20), ALCL(20),
  CLDR(20)
REAL X, U, CU2, CM, BETA, W1, REY
REAL VISC, ASOUND, M, C, ALPHA, BETA2, CD, CL
REAL POP, SIGCL(15), DELTA, P1, P2, PICD(15), P2CD(15), GAMA, RO;
P3CD(15), STAG, ALPHA, PITCH, TEMP(15), ALPCR, RPM, TOR;
CDCR, DBLD(15), DELL, DTOR(15), POW(15), CLCR
STDG, BET2, WM, TEMP5, TEMP6, CD35(20), CD37(20),
CD45(20), CD47(20), CL35(20), CL37(20), CL45(20), CL47(20), AB(15),
DIMENSION FOR THE SECOND STAGE
  
```

1 1 1 2 3 4 5

```

REAL SC(15), SCU2(15), SETA(15), W3(15), SREY(15), SM(15), STAG2(15),
STDC2(15), SDTOR(15), STOR, SETAM(15), SET2(15)
INTEGER I, K, J, L
ALPHA = STDG - STAG + PITCH
CALL CLNEW( ALPHA, M, CD, CL )
CALL CDNEW( CL, M, CD, CL )
GAMA = ATAN( CD / CL )
CALL INDUC( BETA, CL, X, GAMA, C, BETA2 )
ALPHA = BETAM * 180. / 3.1416
BET2 = ALPHA * 180. / 3.1416
ALPHA = ALPHA - ALPHA
ALPCR = ALPHA
CALL CLNEW( ALPCR, M, CD, CLCR )
CALL CDNEW( CLCR, M, CDCR )
  
```

CC

CHANGING THE ATTACK ANGLE

```

WM = SQRT( CM **2 + ( U - .5*CU2 ) **2 )
DELL = RO * WM **2 * 8 / CL
TEMP5 = ATAN( .0 / CL )
BETAM = ATAN( ( U - .5*CU2 ) / CM )
DELF = DELL * COS( TEMP5 ) * COS( BETAM ) - TEMP5 )
WM = SQRT( CM **2 + ( U - .5*CU2 ) **2 )
  
```

CCCCCCCC

```

DELL = RO*WM          **2*CL      *C      *.5
TEMP5 = ATAN(CD      /CL      )
BETAM = ATAN((U      - .5*CU2) / CM      )
DELF  = DELL / COS(TEMP5)*COS(BETAM)  -TEMP5)
WM     = CM / COS(BETAM)
DELL   = RO*WM      **2*CLCR    *C      *.5
TEMP5  = ATAN(CDCR  /CLCR      )
DELF   = DELL / COS(TEMP5)*COS(BETAM)  -TEMP5)
RETURN
END

```

SUBROUTINE TO COMPUTE THE L I F T COEFFICIENT FOR EACH STATION USING NEWTON'S FORWARD AND BACKWARD INTERPOLATION FORMULA GIVEN DATA FORM CURVE CL VS ALPHA FOR MACH NUMBER EQUAL .3 AND .45 OF THE AIRFOIL NACA 16-X12

DESCRIPTION OF PARAMETERS

ALPHA = ANGLE OF ATTACK (DEG.)
 CMAC = MACH NUMBER LESS OR EQUAL 45
 CLM = LIFT COEFFICIENT INTERPOLATED

```

SUBROUTINE CLNEW(ALPHA, CMAC, CLM)
COMMON CL364(20), CL464(20), CD364(20), CD464(20), ALCL(20), CLDR(20)
REAL ALINT(ALPHA, T, CLR3, CLR4, DEL1(20), DEL2(20), DEL3(20), DEL4(20))
INTEGER I, J, K, L
IF (ALPHA + 6.) > 172.73
IF (ALPHA - 12.) < 84.84, 83
WRITE(6, 161) ALPHA IS LESS THAN -6.0 DEGREE'
FORMAT(6, 161) ALPHA IS LARGER THAN 12.0 DEGREE'
ALPHA = -6.0
GO TO 84
WRITE(6, 162) ALPHA IS LARGER THAN 12.0 DEGREE'
FORMAT(6, 162) ALPHA IS LARGER THAN 12.0 DEGREE'
ALPHA = 12.0
ALINT = FIX(ALPHA)
T = ALPHA - ALINT
DO 40 I = 1, 19
IF (ALCL(I) - ALINT) 35, 36, 36
CONTINUE
CONTINUE
IF (I - 12) 41, 41, 42
J = I

```

CCCC

CCCCCCCCCCCCCCCCCCCC

C C BLOCK TO INTERPOLATE POINT IN CL VS ALPHA CURVE USING
 C C NEWTON'S FORWARD INTERPOLATION FORMULA

```

K=1
DO 53 I=1,18
DEL1(I)=CL364(I+1)-CL364(I)
CONTINUE
TEMP1=CL364(J)
DO 60 I=1,17
DEL2(I)=DEL1(I+1)-DEL1(I)
CONTINUE
DO 70 I=1,16
DEL3(I)=DEL2(I+1)-DEL2(I)
CONTINUE
DO 80 I=1,15
DEL4(I)=DEL3(I+1)-DEL3(I)
CONTINUE
CLR(K)={1.+T*DEL1(J)+T*(T-1)*DEL2(J)/2.+T*(T-1)*DEL3(J)/6.+T*(T-1)*DEL4(J)/24.}*TEMP1
DEL3(K-2)}{43,44,44}
IF(K-2) 43,44,44
DO 90 I=1,18
DEL1(I)=CL464(I+1)-CL464(I)
CONTINUE
TEMP1=CL464(J)
K=K+1
GO TO 100
CLR3=CLR(1)
CLR4=CLR(2)
GO TO 51
IF(I-19) 144, 145, 144
J=I
GO TO 146
J=I+1
T=T-1

```

C C BLOCK TO INTERPOLATE POINT IN CL VS ALPHA CURVE USING
 C C NEWTON'S BACKWARD INTERPOLATION FORMULA

```

146 K=1
DO 55 I=1,18
L=20-I
DEL1(L)=CL364(L)-CL364(L-1)
CONTINUE
TEMP1=CL364(J)
DO 65 I=1,17
L=20-I
DEL2(L)=DEL1(L)-DEL1(L-1)
CONTINUE
DO 75 I=1,16

```

```

L=20-I
DEL3(L)=DEL2(L )-DEL2(L-1)
CONTINUE
DO 85 I=1, 15
L=20-I
DEL4(L)=DEL3(L )-DEL3(L-1)
CONTINUE
CLR(K)=(1.+T*DEL1(J)+T*(T-1))*DEL2(J)/2.+T*(T-1.)*TEMP1*(T-2.)*
DEL3(J)/6.+T*(T-1.)*DEL4(J)/24.*TEMP1
IF(K-2) 48,49,49
DO 95 I=1, 18
L=20-I
DEL1(L)=CL464(L )-CL464(L-1)
CONTINUE
TEMP1=CL464(J)
K=K+1
GO TO 105
CLR3=CLR(1)
CLR4=CLR(2)
IF(CMAC-.3) 31,31,33
CLM=CLR3
GO TO 52
CLM=(CLR4-CLR3)/.15*(CMAC-.3)+CLR3
RETURN
END

```

SUBROUTINE TO COMPUTE THE D R A G COEFFICIENT FOR EACH STATION USING NEWTON'S FORWARD AND BACKWARD INTERPOLATION FORMULA, DATA GIVEN FROM CURVE CD VS CL FOR MACH NUMBER EQUAL .3 AND .45 OF AIRFOIL NACA 16-X12

DESCRIPTION OF PARAMETERS

CLM = LIFT COEFFICIENT INTERPOLATED BY SUBROUTINE CLNEW
CMAC = SAME MACH NUMBER USED FOR SUBROUTINE CLNEW
CDM = DRAG COEFFICIENT INTERPOLATED

```

SUBROUTINE CDNEW(CLM CMAC CDM)
COMMON CL364(20),CL464(20),CD364(20),CD464(20),ALCL(20),CLDR(20)
REAL ALINT,ALPHA,T,CLR3,CLR4,DELI(20),DEL2(20),DEL3(20),DEL4(20)
1 TEMPI,CLR(5),CDR(5)
INTEGER I,J,K,L
IF(CLM+.1) 71,72,73

```

CCCCCCCCCCCCCCCCCCCC

```

73 IF(CLM - 1.2 )84,84,83
71 WRITE(6,161) CL IS LESS THAN -.1
72 CLM = -1
GO TO 84
83 WRITE(6,162) CL IS LARGER THAN 1.2
162 FORMAT(
CLM = 1.2
)
84 ALINT=IFIX(CLM*10.)
T=(CLM*10.-ALINT)/10.
DO 40 I=1,14
IF(CLDR(I)-ALINT/10.)35,36,36
CONTINUE
CONTINUE
IF ( I-8 ) 41,41,42
J=I
BLOCK TO INTERPOLATE POINT IN CD VS CL CURVE USING
C NEWTON'S FORWARD INTERPOLATION FORMULA
C
K=1
DO 53 I=1,13
DEL1(I)=CD364(I+1)-CD364(I)
CONTINUE
TEMP1=CD364(J)
DO 60 I=1,12
DEL2(I)=DEL1(I+1)-DEL1(I)
CONTINUE
DO 70 I=1,11
DEL3(I)=DEL2(I+1)-DEL2(I)
CONTINUE
DO 80 I=1,10
DEL4(I)=DEL3(I+1)-DEL3(I)
CONTINUE
CDR(K)=(1.+T**DEL1(J)+T**DEL2(J)+T**DEL3(J)+T**DEL4(J))/2.+T*(T-1.)*TEMP1
DEL3(J)/6.+T*(T-1.)*TEMP1
IF(K-2) 43,44,44
DO 90 I=1,13
DEL1(I)=CD464(I+1)-CD464(I)
CONTINUE
TEMP1=CD464(J)
K=K+1
GO TO 100
44 CDR3=CDR(1)
CDR4=CDR(2)
GO TO 51
42 J=I+1
T=T-.1
C BLOCK TO INTERPOLATE POINT IN CD VS CL CURVE USING
C NEWTON'S BACKWARD INTERPOLATION FORMULA
C

```

C C

```

K=1
DO 55 I=1,13
L=15-I
DEL1(L)=CD364(L) - CD364(L-1)
CONTINUE
TEMP1=CD364(J)
DO 65 I=1,12
L=15-I
DEL2(L)=DEL1(L) - DEL1(L-1)
CONTINUE
DO 75 I=1,11
L=15-I
DEL3(L)=DEL2(L) - DEL2(L-1)
CONTINUE
DO 85 I=1,10
L=15-I
DEL4(L)=DEL3(L) - DEL3(L-1)
CONTINUE
CDR(K)={1.+T*DEL1(J)+T*(T-1)*DEL2(J)/2.+T*(T-1.)*(T-2.)*
DEL3(J)}/6.+T*(T-1.)*(T-2.)*DEL4(J)/24.)*TEMP1
IF(K-2) 48,49,49
DO 95 I=1,13
L=15-I
DEL1(L)=CD464(L) - CD464(L-1)
CONTINUE
TEMP1=CD464(J)
K=K+1
GO TO 105
CDR3=CDR(1)
CDR4=CDR(2)
IF(CMAC-.3) 31,31,33
CDM=CDR3
GO TO 52
CDM=(CDR4-CDR3)/.15*(CMAC-.3)+CDR3
RETURN
END

```

SUBROUTINE TO COMPUTE THE INDUCED ANGLE OF ATTACK AT EACH STATION

DESCRIPTION OF PARAMETERS

CCCCCCCCCCCC

```

BETA = AIR INFLOW ANGLE (RAD.)
CL = LIFT COEFFICIENT
X = STATION POSITION
GAMA = ARC TANGENT OF DRAG COEFFICIENT DIVIDED BY TIP RADIUS
      COEFFICIENT (RAD.)
C = CHORD OF STATION (FT)
BETA2 = LEAVING AIR FLOW ANGLE (RAD.)
ALPHA = INDUCED ANGLE OF ATTACK (RAD.)
BETAM = MEAN VELOCITY ANGLE (RAD.)

```

```

SUBROUTINE INDUC ( BETA, CL, X, GAMA, C, BETA2, ALPHA, BETAM)
REAL X, BETA, CL, GAMA, C, ALPHA, TEMP1, TEMP2, BETA2, BETAM, POP, SIGCL,

```

```

1 INTEGER IN
  DELTA = .1
  ALPHA = -2.*ALPHA
  BETA2 = BETA - 1.57
  IF (BETA2 .GE. 1.57) GO TO 410
  BETAM = BETA - ALPHA
  POP = 2.*(COS(BETAM) ** 2 * COS(GAMA) * (TAN(BETA) - TAN(BETA2))) /
  SIGCL = C * CL * 2. / (3.1416 / 3.75 / X)
  IF (POP .GT. SIGCL) GO TO 409
  GO TO 410
  ALPHA = ALPHA - DELTA
  DELTA = DELTA / 10
  ALPHA = ALPHA + DELTA
  IN = IN + 1
  IF (IN .EQ. 31, 500, 500)
  GO TO 80
  WRITE(6, 15) ALPHA, POP, SIGCL, BETA, BETA2, BETAM, GAMA
  C
  15 FORMAT (7F9.4)
  RETURN
  END

```

MAIN MAIN MAIN PROGRAM

THIS PROGRAM EVALUATES THE POWER PRODUCED BY THE FIRST AND SECOND STAGE OF FAN SYSTEM OF THE LARGE ACADEMIC WIND TUNNEL, AT SPECIFIED PITCH ANGLE OF THE BLADES.

IT IS ITERATIVE, IT ASK YOU IF YOU WANT THE POWER OF FIRST STAGE ONLY OR FOR BOTH. AFTER YOU HAVE TO ENTER THE TEST SECTION VELOCITY AND FINALLY THE INITIAL PITCH ANGLE, THE INCREMENT OF THIS ANGLE AND HOW MANY ITERATIONS DO YOU WANT.

THE INPUT FOR THIS PROGRAM ARE:

VISC = KINEMATIC VISCOSITY
 ASOUND = SOUND VELOCITY (FT/SEC)
 RO = SPECIFIC DENSITY(SLUG/FT3)
 RPM = ROTATIONAL SPEED
 X(I) = LOCAL STATION LOCAL RADIUS DIVIDED BY TIP RADIUS
 C(I) = CHORD FOR FIRST STAGE
 STAG(I) = STAGGER ANGLE FOR FIRST STAGE
 CLDR(I) = LIFT COEFFICIENT USED TO GET DATA FROM CURVE CD VS CL AT NACA TN 1546
 CD35(I) = DRAG COEFFICIENT AT M=.3 AND DESIGN CL = .5
 CD37(I) = DRAG COEFFICIENT AT M=.3 AND DESIGN CL = .7
 CD45(I) = DRAG COEFFICIENT AT M=.45 AND DESIGN CL = .5
 CD47(I) = DRAG COEFFICIENT AT M=.45 AND DESIGN CL = .7
 ALCL(I) = ANGLE OF ATTACK USED TO GET DATA FORM CURVE AT NACA TN 1546
 CL35(I) = LIFT COEFFICIENT AT M= .3 AND DESIGN CL = .5
 CL37(I) = LIFT COEFFICIENT AT M= .3 AND DESIGN CL = .7
 CL45(I) = LIFT COEFFICIENT AT M= .45 AND DESIGN CL = .5
 CL47(I) = LIFT COEFFICIENT AT M= .45 AND DESIGN CL = .7
 SC(I) = CHORD AT STATION FOR SECOND STAGE
 STAG2(I) = STAGGER ANGLE FOR SECOND STAGE

OUTPUT

CD364(I) = DRAG COEFFICIENT AT M= .3 AND DESIGN CL=.64
 CD464(I) = DRAG COEFFICIENT AT M=.45 AND DESIGN CL=.64
 CL364(I) = LIFT COEFFICIENT AT M=.3 AND DESIGN CL=.64
 CL464(I) = LIFT COEFFICIENT AT M=.45 AND DESIGN CL=.64
 DTOR(I) = TORQUE AT STATION OF FIRST STAGE OF BLADES
 TOR(I) = TORQUE FOR THE WHOLE BLADE OF THE FIRST STAGE
 STOR(I) = TORQUE AT STATION OF SECOND STAGE OF BLADES
 del1(I) = lift at station per unit length
 del2(I) = tangential force at station per unit length
 COMMON CL364(20), CL464(20), CD364(20), CD464(20), ALCL(20),
 1 CLDR(20)
 REAL X(15) U(15) CU2(15) CM(15) BETA(15) W1(15) REY(15)
 REAL VISC ASOUND M(15) C(15) ALPHA(15) BETA2(15) CD(15) CL(15)
 1 BETAM(15) POP SIGCL(15) DELTA P1 P2 P1CD(15) P2CD(15) GAMA RO;
 2 P3CD(15) STAG(15) ALPHA(15) PITCH(15) TEMP(15) ALPCR(15) RPM TOR;
 3 CDCR(15) DBLD(15) DELL(15) DTOR(15) POW(15) CLCR(15);
 4 STDG(15) BET2(15) WM(15) TEMP5 TEMP6 TEMP7 CD35(20) CD37(20);
 5 CD45(20) CD47(20) CL35(20) CL37(20) CL45(20) CL47(20) AB(15)
 DIMENSION FOR THE SECOND STAGE

CC

C

```

C      REAL SC(15), SCU2(15), SETA(15), W3(15), SREY(15), SM(15), STAG2(15),
1      STDG2(15), SDTOR(15), STOR, SETAM(15), SET2(15), S, PA, PAL, DPA, V
      INTEGER I, K, J, L, NPA
      READ (5, 30) VISC, ASOUND, RO, RPM
30      FORMAT (5F10.5, 2X)
      READ (5, 20) (X(I), C(I), STAG(I), I=1, 11)
20      FORMAT (3F10.5)
10      READ (5, 10) (CLDR(I), CD35(I), CD37(I), CD45(I), CD47(I), I=1, 14)
      FORMAT (5F10.5)
C      WRITE (6, 7) (CLDR(I), CD35(I), CD37(I), CD45(I), CD47(I), I=1, 14)
C      FORMAT (5F10.5)
11      READ (5, 11) (ALCL(I), CL35(I), CL37(I), CL45(I), CL47(I), I=1, 19)
      FORMAT (5F10.5)
600     READ (5, 600) (SC(I), STAG2(I), I=1, 11)
      FORMAT (2F10.5)
      PRINT, 'EVALUATION FOR FIRST STAGE ENTER 1'
      PRINT, 'EVALUATION FOR BOTH STAGE ENTER 2'
      PRINT, S
      PRINT, V
      READ, Y
      PRINT, 'ENTER INITIAL, THE INCREMENT AND THE NUMBER OF INTERVAL'
      PRINT, 'OF PITCH ANGLE. SAMPLE 2.5, .5, 6'
      READ, PAL, DPA, NPA
      PA=PAL-DPA
      DO 587 I=1, NPA
      PA=PA+DPA
      PITCH(I)=PA
      CONTINUE
587     WRITE (6, 6) (ALCL(I), CL35(I), CL37(I), CL45(I), CL47(I), I=1, 19)
      FORMAT (5F10.5)
C      WRITE (6, 21) VISC, ASOUND, RO, RPM
C      FORMAT (7F10.5, 2X)
C      WRITE (6, 21) VISC, ASOUND, 'F12.6, 2X, 'RO=' , F12.6,
C      2X, RDS= , F12.6)
C      DO 15 I=1, 19
C      CL364(I)=.7*CL37(I)+.3*CL35(I)
C      CL464(I)=.7*CL47(I)+.3*CL45(I)
C      CONTINUE
15     DO 22 I=1, 14
      CD364(I)=.7*CD37(I)+.3*CD35(I)
      CD464(I)=.7*CD47(I)+.3*CD45(I)
      CONTINUE
22     WRITE (6, 3) (CLDR(I), CD364(I), CD35(I), CD47(I), CD464(I),
      CD45(I), I=1, 14)
      FORMAT (7F10.5, 2X, F8.4)
C      WRITE (6, 2) (ALCL(I), CL37(I), CL35(I), CL47(I), CL464(I),
      CL45(I), I=1, 19)
      FORMAT (7F10.5, 2X, F8.4)
C      2

```

```

DO 50 I=1,11
CALL FIRST(X(I),V,C(I),ASOUND,VISC,CM(I),CU2(I),U(I),BETA(I),
1 W1(I),REY(I),M(I))
1 STDG(I)=BETA(I)*180.0/3.1416
50 CONTINUE
C
WRITE(6,60)
60 FORMAT(//,5X,'STATION',7X,'CHORD',10X,'U',9X,'CU2',9X,'CM',8X,
1 BETAI(6,170)(X(I),C(I),U(I),CU2(I),CM(I),STDG(I),W1(I),I=1,11)
170 WRITE(6,60)
271 FORMAT(6X,STATION',9X,'REY',8X,'MACH',9X,'STAG')
271 WRITE(6,160)(X(I),REY(I),M(I),STAG(I),
160 FORMAT(4F13.3)
I=1,11)
C

```

```

DO 70 K=1,NPA
TOR=0
WRITE(6,16)
16 FORMAT(//,3X,'ALPHAI',4X,'POP',5X,'SIGCL',4X,'BETA1',4X,
1 'BETA2',4X,'BETAM',4X,'GAMA')
C

```

```

DO 71 I=1,11
ALPHA(I)=STDG(I)-STAG(I)+PITCH(K)
CALL CLNEW( ALPHA(I),M(I),CL(I))
CALL CDNEW( CL(I),M(I),CD(I))
GAMA=ATAN(CD(I)/CL(I))
CALL INDUC( BETA(I),X(I),GAMA,C(I),BETA2(I),
1 ALPHA(I),BETAM(I))
ALPHA(I)=BETA2(I)*180./3.1416
ALPHA(I)=ALPHA(I)-ALPHAI(I)
ALPCR(I)=ALPHA(I)-ALPHAI(I)
CALL CLNEW(ALPCR(I),M(I),CLCR(I))
CALL CDNEW(CLCR(I),M(I),CDCR(I))
C

```

CHANGING THE ATTACK ANGLE

```

WM(I)=SQRT(CM(I)**2+(U(I)-.5*CU2(I))**2)
DELL(I)=RO*WM(I)**2*.8/CL(I)*.5
TEMP5=ATAN(.0/CL(I))
BETAM(I)=ATAN((U(I)-.5*CU2(I))/CM(I))
DELF(I)=DELL(I)/COS(TEMP5)*COS(BETAM(I)-TEMP5)
WM(I)=SQRT(CM(I)**2+(U(I)-.5*CU2(I))**2)
DELL(I)=RO*WM(I)**2*.8/CL(I)*.5
TEMP5=ATAN(CD(I)/CL(I))
BETAM(I)=ATAN((U(I)-.5*CU2(I))/CM(I))
DELF(I)=DELL(I)/COS(TEMP5)*COS(BETAM(I)-TEMP5)
WM(I)=CM(I)/COS(BETAM(I))
C

```



```

660 WRITE(6,660) S F C O N D $ T A G F P A R A M E T E R S '
      FORMAT(//,STATION',7X,'CHORD',6X,U',9X,SCU2',9X,CM',8X,
      'BETA3',8X,W3)
      WRITE(6,670)(X(I),SC(I),U(I),SCU2(I),CM(I),STDG2(I),W3(I),
      I=1,11)
      FORMAT(//,7F12.5)
670
671 WRITE(6,671)STATION',9X,'REV',8X,'MACH',9X,'STAG2'
      WRITE(6,680)(X(I),SREY(I),SM(I),STAG2(I),I=1,11)
      FORMAT(4F13.3)
C
DO 604 L=1,NPA
DO 605 I=1,11
CALL LIFT(STDG2(I),STAG2(I),PITCH(L),SM(I),SETA(I),X(I),SC(I),
CM(I),U(I),SCU2(I),RO,DELF(I),SETAM(I),SET2(I),ALPHAI(I),
ALPHA(I),CL(I),CD(I),ALPCR(I),CLCR(I),CDCR(I),DELL(I))
PICD(I)=STDG(I)-SET2(I)
CONTINUE
C
DO 673 I=1,10
STOR=0
TEMP5=(X(I+1)-X(I))*3.75
TEMP6=(DELF(I)+DELF(I+1))/2.
TEMP7=(X(I)+X(I+1))/2.*3.75
SDTOR(I)=TEMP6*TEMP7*TEMP5
STOR=STOR+SDTOR(I)
CONTINUE
C
673
POW(L)=STOR*RPM/550.*4
WRITE(6,691) L,PITCH(L),POW(L)
FORMAT(//,K=,I4,THE PITCH ANGLE IS =',F8.2,
POWER=',F15.6)
C
691
WRITE(6,690)STATION',3X,'BETA3',3X,'BETA4',3X,'BETAM2',3X,
FORMAT(//,3X,'ALPHAI',4X,'ALPHA',4X,'CL',4X,'CD')
STAG2 4X,ALPHAI,4X,ALPHA,4X,CL,4X,CD)
DO 683 I=1,11
SETAM(I)=SETAM(I)*180/3.1416
WRITE(6,800)(X(I),STDG2(I),SET2(I),STAG(I),ALPHAI(I),
ALPHA(I),CL(I),CD(I),I=1,11)
FORMAT(9F9.3)
C
800
WRITE(6,802)STATION',5X,'ALPCR',7X,'CLCR',9X,'CDCR',9X,
FORMAT(//,5X,'DTOR',7X,'BETA1-BETA4',7X,
DELL(BETA4),7X,BETA1-BETA4,7X,
DELL(BETA4),7X,BETA1-BETA4,7X,
X(I),ALPCR(I),CLCR(I),CDCR(I),DELL(I),PICD(I),
SDTOR(I),I=1,11)
FORMAT(7F12.5)
C
801
CONTINUE
C

```

```

C 70 CONTINUE
C
C 302 WRITE(6,302) CM CORRECTED CL CONSTANT
C 301 FORMAT(/,301)(POW(I),I=1,11)
C 304 WRITE(6,304)((BT(K,I),I=1,11),K=1,11)
C 161 FORMAT(6F10.7,/5F10.7)
C
C 161 RETURN
C 161 END
$ENTRY
000166 1.1118 1160.35 58 .0023 125.6637 0 0
.267 1.10485 40.37
.35 .9579 46.67
.4 .8753 51.77
.45 .8018 56.03
.5 .7378 59.65
.6 .6705 65.33
.7 .6163 69.59
.8 .5711 72.85
.9 .5348 75.42
1. .5043 77.45
.1 .4821
.2 .4642
.3 .4501
.4 .4401
.5 .4338
.6 .4301
.7 .4281
.8 .4267
.9 .4257
1. .4251
1.1 .4248
1.2 .4246
1.6 .4244
2. .4243
3. .4242
4. .4241
0 1.19 285
1 2.365
2 4.46
3 5.535
4 6.567

```

.93
.96
1.09
1.14
1.18
1.18

.74
.79
.85
.94
1.0
1.0

.915
.93
.97
1.04
1.085
1.14
1.18
1.2

.735
.765
.84
.91
.965
1.01
1.05
1.07
46.61
49.28
53.10
56.61
59.76
62.09
67.02
70.72
73.58
75.88
77.88

5.
6.
7.
8.
9.
10.
11.
12.
931
.895
.834
.777
.724
.673
.5897
.519
.461
.373

LIST OF REFERENCES

1. Borst, Henry V. A New Blade Element Method for Calculating the Performance of High and Intermediate Solidity Axial Flow Fans, NASA Contractor Reporter 3063, Nov, 1978.
2. Rae Jr., William H. and Pope, Alan, Low - Speed Wind Tunnel Testing, Wiley - Interscience, 1984.
3. Pankhurst, R. C. and Holder, D. W., Wind - Tunnel Technique, Sir Isaac Pitman & Sons, Ltd, 1952.
4. Larson, First and Second Blade Stage Design Report, 5/20/57, West Coast Research Co.
5. Bradshaw, P. and Pankhurst, R. C., The Design of Low - Speed Wind Tunnels, Progress in Aeronautical Sciences, Vol 5, 1984.
6. Eckert, William T., Mort, Kenneth W. and Poje, Jean, Aerodynamic Design Guidelines and Computer Program for Estimation of Subsonic Wind Tunnel Performance, NASA Technical Note - NASA TN-D-8243, 1976.
7. Drawing - Assy Vanes, Turning Academic Wind Tunnel No 656 - 501, Version B, 7/23/57, West Coast Research Co. Los Angeles 64, California.
8. Drawing - Proposal Academic Wind Tunnel Facility, No 2, 12/7/55, West Coast Research Co. Los Angeles 64, California.
9. Drawing - Blades Drawing, First and Second Fan Stages, 7/15/57, West Coast Research Co., Los Angeles 64, California.
10. Nicolai, Leland N., Fundamentals of Aircraft Design, Mets, Inc., 6520 Kingsland Court, San Jose, Ca, 95120, Revised 1984.
11. Osborne, William C., Fans, 2nd Edition (in SI/ Metric Units), Pergamon Press Inc., Maxwell House, Fairview Park, Elmsford, New York, 10523, USA, Second Edition 1977.
12. Lindsey, W. F., Stevenson, D. B. and Daley, Bernard N., Aerodynamic Characteristics of 24 Naca 16 - Series Airfoils at Mach Numbers Between 0.3 and 0.8 - NACA TN No 1546, 1947.

INITIAL DISTRIBUTION LIST

	No. Copies
1. Defense Technical Information Center Cameron Station Alexandria, Virginia 22304-6145	2
2. Library, Code 0142 Naval Postgraduate School Monterey, California 93943	2
3. Department Chairman, Code 67 Department of Aeronautical Engineering Naval Postgraduate School Monterey, California 93943	1
4. J. V. Healey, Code 67X1 Department of Aeronautical Engineering Naval Postgraduate School Monterey, California 93943	1
5. Centro Tecnico Aeroespacial Rua Paraibuna S/N 12225 Sao Jose dos Campos-SP Sao Paulo, BRAZIL	1
6. Centro Tecnico Aeroespacial Instituto de Atividades Espaciais Rua Paraibuna S/N 12225 Sao Jose dos Campos, SP Sao Paulo, BRAZIL	2
7. Centro Tecnico Aeroespacial Instituto de Atividades Espaciais Divisao de Sistemas Belicos Rua Paraibuna S/N 12225 Sao Jose dos Campos, SP Sao Paulo, BRAZIL	2
8. Lt.Col. Marcos Luis Pereira Centro Tecnico Aeroespacial Instituto de Atividades Espaciais Rua Paraibuna S/N 12225 Sao Jose dos Campos, SP Sao Paulo, BRAZIL	3

END

FILMED

3-86

DTIC